Accepted Manuscript

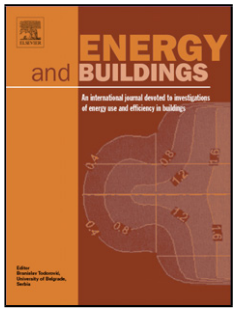

Title: Floor heating and cooling combined with displacement ventilation: possibilities and limitations

Authors: Francesco Causone, Fabio Baldin, Bjarne W. Olesen, Stefano P. Corgnati

PII: S0378-7788(10)00260-4
DOI: doi:10.1016/j.enbuild.2010.08.001
Reference: ENB 2938

To appear in: *ENB*

Received date: 23-4-2009
Revised date: 21-7-2010
Accepted date: 5-8-2010

Please cite this article as: F. Causone, F. Baldin, B.W. Olesen, S.P. Corgnati, Floor heating and cooling combined with displacement ventilation: possibilities and limitations, *Energy and Buildings* (2008), doi:10.1016/j.enbuild.2010.08.001

This is a PDF file of an unedited manuscript that has been accepted for publication. As a service to our customers we are providing this early version of the manuscript. The manuscript will undergo copyediting, typesetting, and review of the resulting proof before it is published in its final form. Please note that during the production process errors may be discovered which could affect the content, and all legal disclaimers that apply to the journal pertain.

Manuscript
ACCEPTED MANUSCRIPT

Floor heating and cooling combined with displacement ventilation: possibilities and limitations

Francesco Causone[1,*], Fabio Baldin[2], Bjarne W. Olesen[3], Stefano P. Corgnati[1]

[1]*TEBE Research Group, Department of Energetics, Politecnico di Torino, Corso Duca degli Abruzzi 24 – 10129 Torino, Italy*

[2]*Department of Applied Physics, University of Padova, via Venezia 1 – 35131 Padova, Italy*

[3]*ICIEE, Department of Civil Engineering, Technical University of Denmark, Nils Koppels Allé Building 402 – 2800 Kgs. Lyngby, Denmark*

∗ Corresponding author: tel.: +39 011 090 4430; fax: +39 011 090 4499; e-mail address: francesco.causone@polito.it

Abstract

Design guidelines envisage that floor heating can be used together with displacement ventilation (DV), provided that the supply air is not overly heated before it can reach heat and contaminant sources. If this is not controlled a mixing flow pattern could occur in the room. The use of floor cooling with DV is also considered possible, although draught risk at ankle level and vertical air temperature differences must be controlled carefully, because they could increase.

Few studies on these topics were found in the literature.

An indoor environmental chamber was set up to obtain measurements aimed at analysing the possibilities and limitations of combining floor heating/cooling with DV. Air temperature profiles, air velocity profiles, surface temperatures and ventilation effectiveness were measured under different environmental conditions that may occur in practice. These values were compared to equivalent temperature measurements obtained using a thermal manikin.

The measurements show that floor heating can be used with DV, obtaining high ventilation effectiveness values. A correlation between the floor heating capacity and the air temperature profile in the room was found. Measurements showed that floor cooling does not increase draught risk at ankle level, although it does increase vertical air temperature differences.

Accepted Manuscript

ACCEPTED MANUSCRIPT

Keywords: floor heating, floor cooling, displacement ventilation, DV, thermal comfort, hybrid systems

1. Introduction

Radiant floor heating and radiant floor cooling are becoming common in residential, commercial and industrial buildings, because of the comfort advantages and the energy saving opportunities they can provide [1- 4]. *As there have already been extensive studies of the energy saving potential of the proper use of radiant heating/cooling [5-14], the focus of the present paper is on a different and specific topic: the thermal comfort and ventilation effectiveness that can be achieved by combining radiant floor heating/cooling with displacement ventilation.*

A heating/cooling system must ensure an acceptable thermal environment for occupants both in terms of whole-body thermal comfort (PMV, PPD, operative temperature) and in terms of local thermal comfort (floor temperature, vertical air temperature differences, radiant temperature asymmetries, draught). Radiant floors provide homogeneous thermal conditions inside rooms, reducing vertical air temperature differences and radiant temperature asymmetries, because they exchange heat with the surroundings (walls, furniture, occupants and air) by radiation and by convection in similar amounts [15].

The high level of radiant heat transfer between a floor and the occupants and the surrounding surfaces, makes it possible to reduce the room air temperature in the heating season and to increase it in the cooling season while still maintaining the required level of operative temperature. Ventilation heat losses in the heating season and ventilation heat gains in the cooling season are then reduced, ensuring energy saving together with a high level of thermal comfort. Furthermore, the draught risk due to cold air movement can be reduced by using floor cooling, in comparison with other mainly convective systems, because ventilation air can be supplied at a higher temperature [1, 2].

When a radiant floor is used, a suitable floor temperature can be maintained (19 – 29 °C), so the use of carpets is not necessary. Since carpets have been found to be one of the main pollutant sources in rooms, the use of a radiant floor may reduce pollutant levels inside buildings [2]. Radiant floors also generate low air movements and consequently low dust movements, further improving indoor air quality [1, 2]. With radiant floors, the entire floor area can then be freely used, ensuring an efficient use of space and no limitations on architectural design or occupant use.

Accepted Manuscript

ACCEPTED MANUSCRIPT

Compared to other radiant systems currently in use, floor heating/cooling has the highest angle factor to the occupants. It can therefore provide a high level of thermal comfort with lower surface temperatures in the heating season and higher surface temperatures in the cooling season [1, 2].

An air ventilation system must nevertheless be operated together with a radiant floor, because radiant systems cannot provide control of the latent heat load. Additionally, minimum ventilation rates for air renewal and indoor air quality are mandatory for commercial and industrial buildings and necessary in new airtight residential buildings.

When comparing ventilation strategies, displacement ventilation is regarded as one of the most interesting solutions, because it can provide high air quality levels at the breathing level [*16*]. By exploiting buoyancy forces in the room, displacement ventilation generates a stratified flow pattern: the warm and polluted air is concentrated in the upper part of the room, while the cool and clean air remains in the lower part of the room where the occupants are located [*17, 18*]. Displacement ventilation can therefore provide ventilation effectiveness values up to 1.4 (or more under laboratory conditions), while mixing ventilation provides ventilation effectiveness values only up to 1 [*19*], even in theory, and in practice fall well short of this maximum level, due to short-circuiting.

The possibilities and limitations of combining radiant ceilings with displacement ventilation have been widely studied [*20-24*]. In contrast, few scientific studies of the possibilities and limitations of combining radiant floors with displacement ventilation are available [*25, 26*]. *Radiant floor cooling combined with displacement ventilation is used in the new Bangkok airport, whose innovative design concept is described in some recent papers [3, 27, 28].*

Radiant floor heating systems produce thermal environments with low vertical air temperature differences, while displacement ventilation produces highly stratified conditions. The main problem encountered when combining radiant floor heating with displacement ventilation is the opposite effects of the two systems. If the floor temperature is too high it could heat the supply air and make it rise, reducing the ventilation effectiveness of the system and producing a mixing flow pattern in the room. Skistad demonstrated, using calculations based on an analytical model, that under typical heat demand conditions this phenomenon should not occur and supply air should spread normally along the floor [*25*].

The use of floor cooling with displacement ventilation may exacerbate the typical problems encountered with displacement ventilation: draught risk at ankle level and discomfort due to the excessive vertical air

Accepted Manuscript

ACCEPTED MANUSCRIPT

temperature differences [*16*]. In the Bangkok airport, under extreme boundary conditions, these problems were avoided by using an accurate design process [3, *27*].

The object of the present study was to evaluate, by means of experimental tests, the possibilities and limitations of combining radiant floor heating and cooling with displacement ventilation. A typical office layout was simulated in an indoor environment chamber equipped with a radiant floor, a wall displacement terminal device and eight plastic plates positioned together on a wall to simulate vertical cold or warm window surfaces. Air temperature profiles, air velocity profiles, surface temperatures and ventilation effectiveness were measured under different boundary conditions and thermal comfort evaluations were obtained by using a thermal manikin.

2. Experimental apparatus

2.1 Indoor environmental chamber

The measurements were carried out in indoor environmental chamber nr.5 at the International Centre for Indoor Environment and Energy, Technical University of Denmark [*29*].

This chamber and two other chambers were specifically designed for experiments on thermal comfort and air quality. It has a net floor/ceiling area of 16.80 m^2 (4.20 m × 4.00 m) and a net internal height of 2.40 m, when a radiant floor is installed (Fig. 1). It is situated in a tall experimental hall with a stable, but not controlled, temperature.

The chamber is thermally insulated and it has walls with a heat transmission coefficient of 0.25 W m^{-2} K^{-1}, to minimize heat exchange with the surrounding space. It is equipped with a ventilation system able to provide airflow rates between 12 and 170 l s^{-1}. The air supplied to the chamber can be heated or cooled in the temperature range between 10 and 40°C and the exhaust system maintains a small overpressure in the chamber.

During the measurements, a wall displacement air terminal device was used, positioned on the symmetry axis of the chamber. The exhaust air terminal device was positioned approximately in the centre of the ceiling.

Accepted Manuscript

ACCEPTED MANUSCRIPT

Ten hydronic radiant heating/cooling panels were positioned over the chamber floor, separated from it by a layer of insulating boards 50 mm thick. Each panel was constructed to have three layers (listed lower to upper): a wooden frame 12 mm thick, an insulation layer 15 mm thick and an aluminium plate 3 mm thick. The panels had an internal piping system: the pipes were in contact with the aluminium plate through a heat conducting metal foil. The aluminium plates were chosen to have a uniform surface temperature distribution and they were painted with a grey opaque overcoat, to obtain a radiant heat transfer coefficient typical of other common finishing materials such as stone, ceramic and plastic floor tiles.

During the measurements, the three windows of the chamber, on the left side of the supply air terminal device, were covered on the external side by means of insulating boards. A small section of the insulating board on the central window could be removed to check measurements.

In order to simulate heat gains and heat losses due to a glazed façade, eight radiant heating/cooling plastic plates were positioned on the wall opposite the supply air terminal device, with a total area of 8.50 m^2.

The chamber was set up to reproduce an office: two desks, two chairs, two desk lights and two PCs were positioned with a symmetrical layout inside the occupied zone; a thermal manikin and a heated dummy were used to reproduce occupant heat loads (Fig. 2).

[place Figure 1 approximately here]

[place Figure 2 approximately here]

2.2 Thermistor Sensors (TS)

Surface temperatures and air temperatures measurements were carried out using fifty-nine thermistor sensors *(Craftemp type).*

The sensors were connected to a single ended relay multiplexer with fifty-nine channels. The multiplexer was connected to a data-logger *type HP 3852A data acquisition/control unit.*

The sensors used are flat and can therefore be attached so that they have good thermal contact with a surface.

Accepted Manuscript

ACCEPTED MANUSCRIPT

The sensors used for air temperature profiles measurements were attached at several heights to a vertical steel bar: 0.03 m, 0.05 m, 0.10 m, 0.15 m, 0.20 m, 0.30 m, 0.60 m, 0.85 m, 1.10 m, 1.40 m, 1.70 m , 2.00 m, 2.30 m. Each sensor was shielded by a small aluminium layer to minimise the effect of long wave radiation exchange.

The thermistor sensors were calibrated in the range between 15°C and 35°C, in order to assure an acceptable accuracy of temperature measurements. After applying the derived software correction the accuracy of the probes was ±0.3°C, within this temperature range.

2.3 Anemometers

Air velocity measurements were carried out by means of nine omnidirectional hot sphere anemometers *(Dantec)*, attached at several heights to a vertical steel bar: 0.03 m, 0.05 m, 0.10 m, 0.15 m, 0.20 m, 0.30 m, 0.60 m, 1.10 m, 1.40 m above the floor. The anemometers were connected to a control unit multichannel flow analyser *(Dantec 54N10).* The mean air velocity and turbulence intensity were measured using an integration time of three minutes. The anemometers had been calibrated using a dedicated wind tunnel *in the range between 0.02 m/s and 2.82 m/s, achieving an uncertainty of ±(0.02 + 0.02 x) m/s, where x is the actual measurement.*

2.4 Tracer gas

Ventilation effectiveness measurements were carried out using CO_2 as a tracer gas. The gas dosing and concentration measurements in the chamber were carried out using a photo-acoustic multi-gas monitor *(Innova 1312).* The measuring device was placed outside the chamber and samples of air were withdrawn from the room through small plastic pipes placed inside the chamber at different heights and locations. Another pipe was used to release CO_2 from the heated dummy, in order to simulate a pollutant associated to a heat source (an occupant). The tracer gas concentration measurements were taken in the air supply duct, in the exhaust duct, in two positions inside the chamber at several heights and outside the chamber. The concentration of the tracer gas was measured also in the hall outside the chamber, in order to determine whether any leakage or infiltration could influence measurements.

Accepted Manuscript

ACCEPTED MANUSCRIPT

The tracer gas concentration values were evaluated in steady state conditions from the average value of ten measurements for each point.

2.5 Thermal manikin

A thermal manikin, composed by seventeen body parts, was used to carry out thermal comfort evaluations. The manikin was calibrated and the heat transfer coefficient of each body part was calculated.

Thermal sensation is closely related to the rate of heat transfer between the human body and surroundings [*30*]. By using a thermal manikin it is possible to calculate the equivalent temperature of each body part, which is a recognised measure of the effects of dry heat loss from the human body [*31, 32*].

When the equivalent temperature values of different body parts are closely similar, a comfortable thermal condition exists inside the chamber, as equivalent temperature differences indicate the presence of radiant asymmetries, draught or high vertical air temperature differences.

2.6 Smoke generator

A smoke generator was used to carry out smoke tests, in order to visualise the airflow pattern in the chamber under different boundary conditions.

3. Experimental programme

3.1 Boundary conditions

Since the chamber layout was symmetrical and the supply air terminal device was positioned on the symmetry axis, measurements were made in only half of the chamber, assuming that symmetrical conditions would occur on the other half of the room. CFD analyses confirmed this assumption *[33].*

Accepted Manuscript

ACCEPTED MANUSCRIPT

The assumption of symmetry made it possible to reduce measurement times, because measurements were carried out under steady state conditions for nine combinations of boundary conditions with floor heating and ten combinations of boundary conditions with floor cooling (Tab. 1, 2).

Ventilation airflow rates were established according to EN standard 15251 [*34*]. For a non-low polluting building in Category I, the recommended ventilation rate is 3 l s^{-1} m^{-2}, while for the same kind of building in Category II the recommended ventilation rate is 2.1 l s^{-1} m^{-2}. Both of these conditions were studied and so ventilation rates of 35 l s^{-1} and 50 l s^{-1} were used. During floor cooling tests a further ventilation rate of 80 l s^{-1} was considered, in order to study the case in which displacement ventilation could balance heat gains without the need for a radiant floor (C5).

[place Table 1 approximately here]

[place Table 2 approximately here]

3.2 Air temperature and air velocity measurements

Thirteen temperature sensors, attached to a movable vertical bar, were used to measure vertical air temperature profiles and nine anemometers, attached to another movable vertical bar, were used to measure air velocity profiles.

The measurements were carried out at the same time, moving the two vertical bars to seven different positions (Fig. 3; Points S1 – S7) in order to be able to adequately describe the air distribution in the chamber.

The data were recorded under steady state conditions and average values were then calculated. The position of the two bars was changed until both velocity measurements and temperature measurements had been concluded for all points. It was found that the chamber needed fifteen minutes to re-establish steady state conditions after each movement of the bars.

Accepted Manuscript

ACCEPTED MANUSCRIPT

3.3 Surface temperature measurements

Unheated walls A and B (Fig. 3) were divided into four sections, each monitored with a temperature sensor. The wall where the supply air terminal device was positioned was also divided in four sections, but only two of them were monitored in accordance with the symmetry assumption noted in Section 3.1 (Fig. 4).

The ceiling surface was divided into six sections, because its temperature has a fundamental role in increasing the temperature of the supply air at floor level. A warm ceiling exchanges heat by means of radiation with the cooler floor, which transfers it to the air at floor level by convection, as described by Elisabeth Mundt [*17, 35*]. Only four of the six sections were monitored, according to the symmetry assumption (Fig. 4).

The surface temperature of the heated or cooled window panels were monitored by means of eight temperature sensors (Fig. 5).

The floor surface was divided in three main sections (Fig. 5). The first section consisted of the panels close to the supply air terminal device, which were within the adjacent zone and therefore were influenced by the higher velocities and lower temperatures of the airflow. This part was monitored by six temperature sensors.

The second part consisted of the panels in the centre of the chamber, those closest to the occupied zone. This section was monitored by five temperature sensors (one of them located under the floor panels to estimate downward heat losses).

The third section was close to the plastic plates simulating windows, so it was influenced by the downdraught, during the floor heating measurements (cold windows) and by the thermal plume, during the floor cooling measurements (warm windows). This part was monitored by nine temperature sensors (one of them located under the floor panels, to estimate downward heat losses).

[place Figure 3 approximately here]

[place Figure 4 approximately here]

[place Figure 5 approximately here]

Accepted Manuscript

ACCEPTED MANUSCRIPT

3.4 Ventilation effectiveness measurements

The concentration of the tracer gas was measured in the air supply duct, in the exhaust duct and at two positions inside the occupied zone (P1 and P2 in Fig. 6). In these two positions the CO_2 concentration was measured at the following heights: 1.10 m, 1.40 m and 1.70 m and in particular cases even at 0.60 m and 0.85 m. By using these data, the ventilation effectiveness could be calculated at each point from the following equation:

$$\varepsilon = \frac{c_e - c_s}{c_j - c_s} \quad (1)$$

The vertical distribution of the ventilation effectiveness values was useful to evaluate the displacement ventilation system efficiency under the different boundary conditions.

[place Figure 6 approximately here]

3.5 Equivalent temperature measurements

During the measurements, the thermal manikin was set to comfort mode and the skin temperature and heat loss of each body part were logged. In comfort mode, the surface temperature of the manikin is controlled to be equal to the skin temperature of an average person in a condition of neutral thermal comfort, in which total heat loss is equal to metabolic heat production.

Using the heat transfer coefficients calculated from the calibration of the manikin, it was possible to calculate the equivalent temperature of each body part, by using the equation:

$$T_{eq} = T_{sk} - \frac{Q_j}{h_j} \quad (2)$$

ACCEPTED MANUSCRIPT

During floor heating tests, the manikin was wearing winter clothing with a total insulation value of 0.8 clo, while during floor cooling tests it was wearing summer clothing with a value of 0.5 clo.
The skin temperature and the heat loss measurements were carried out together with the air velocity and the temperature profiles measurements, in order to obtain comparable data.

3.6 Smoke tests

The smoke generator was connected to the supply air terminal device in order to spread the smoke together with the ventilation air and to follow its path inside the chamber. By means of these tests the airflow pattern inside the chamber was visualised under different boundary conditions.
The smoke always spread along the floor and rose only when it was in contact with some heat source (thermal manikin, dummy, PCs, lights).
Smoke tests were also used to visualise the downdraught due to the cooled windows during floor heating measurements and the thermal plume due to the heated windows during floor cooling tests. The smoke tests were also useful for visualising a particular problem noticed during measurements at Point S7, caused by the heat plumes generated by the legs of the manikin and the legs of the heated dummy.

4. Results

4.1 Air temperature measurements

4.1.1 Floor heating

The air temperature profiles obtained in all nine floor heating cases were analysed and the temperature profiles at Point S4 were taken as the reference for the occupied zone conditions.
The temperatures at Points S1, S2, S3, S7 were influenced by the cool downdraught from the cooled windows; while the temperatures at Points S5 and S6 were influenced by the cool air coming from the terminal device, because they were still in the adjacent zone or close to it.
The measurements show that there is a relation between floor temperature and the thermal stratification in the chamber. At higher floor temperatures (i.e., higher heating input) the air close to the floor surface

Accepted Manuscript

ACCEPTED MANUSCRIPT

warms up faster and a lower vertical air temperature gradient develops in the chamber. There is a close relationship between the dimensionless temperature of the air near the floor (k) and the temperature difference between the floor surface and the operative temperature in the room, as shown in Fig. 7.

$$k = \frac{T_f - T_s}{T_e - T_s} \quad (3)$$

It is worth noting that when passing from no floor heating capacity to a floor heating capacity of 60 W m^{-2}, the dimensionless temperature of the air near the floor changes from 0.5 to 0.8. All of the conditions examined were in this range (Figs. 8 and 9).

Typically, in rooms equipped with displacement ventilation, the "50%-rule" is used as a first approximation to describe the vertical air temperature distribution. *The model known as the "50%-rule" was proposed by Skistad [36]. It postulates that the air temperature at floor level is half-way between the supply air temperature and the extract air temperature and that the air temperature gradient from floor to ceiling level can be considered linear:*

$$\frac{T_f - T_s}{T_e - T_s} = 0.5 \quad (4)$$

If floor heating is used together with displacement ventilation, the "50%-rule" must be changed as a function of the floor heating capacity (Figs. 7 and 9), reaching a maximum at the "80%-rule", corresponding to a floor heating capacity close to 60 W m^{-2}. *The "80%-rule" can be expressed by the analytical expression*:

$$\frac{T_f - T_s}{T_e - T_s} = 0.8 \quad (5)$$

When floor heating with "high" heating capacity is used, the supply air is significantly warmed both by the induction of the room air into the supply airflow and by convective heat transfer with the floor

Accepted Manuscript

ACCEPTED MANUSCRIPT

surface, before reaching occupants and other heat sources. Under these conditions there will be less thermal stratification.

These conclusions are valid for the air supply temperature range used (14°C – 18°C), and thus for temperature differences between supply air and floor surface measured in the range 4°C – 14°C. These are typical design values.

[place Figure 7 approximately here]

[place Figure 8 approximately here]

[place Figure 9 approximately here]

The vertical air temperature profile in Case H7 was much closer to the "50%-rule" profile because the floor temperature, and thus the floor heating capacity, was very low. In this case the transmission losses and the ventilation losses were low and they were balanced by the internal heat gains (manikin, dummy, lights…).

The vertical air temperature profile in Case H9 follows a broken line: between floor level and 1.10 m there was a higher thermal gradient, while between 1.10 m and the ceiling level the thermal gradient was lower. This is the typical profile in rooms where heat sources are located in the lower part of the volume [*16*]. In Case H9 the floor was neutral to the other wall surfaces and it was heating the supply air at the floor level only slightly. The temperature gradient in the room was mainly due to the internal heat gains (manikin, dummy, lights…). The air temperature profile is in fact typical of a room with an unheated floor and displacement ventilation.

If floor heating was used alone, vertical air temperature profiles would have been almost a vertical straight line. During measurements, when displacement ventilation and floor heating were used together, a situation between the extremes described above was registered.

In Case H9 the floor temperature was slightly higher that in Case H7, because the panels simulating windows were not cooled. There was no cold downdraught to cool the floor and a lower radiant heat exchanged occurred between the floor and the panels. Additionally, in Case H9 the room temperature was set at 22°C while in Case H7 it was set at 20°C. All the other wall temperatures were also slightly higher in Case H9 with respect to Case H7, and thermal stratification was found.

Accepted Manuscript

ACCEPTED MANUSCRIPT

Different air temperature profiles were noticed at different positions in the chamber, in all the tests (Fig. 10). At Points S5 and S6, the closest to the supply air device, the vertical air temperature differences are higher, as well at Points S1, S2, S3 and S7, which were influenced by the cool downdraught.

When floor heating was used together with displacement ventilation, the thermal stratification inside the chamber was not as homogeneous as in the case of displacement ventilation without radiant floor. The dimensionless temperatures of the air near the floor in the different positions of the chamber are reported in Table 3. These values make it possible to understand the influence of the supply air or of the downdraught at the different points, compared to the occupied zone (Point S4).

During all the measurements, with the exclusion of Case H9, the vertical air temperature difference between head and ankles was always lower than 2°C (Tab. 4), remaining within the limitations for all categories in ISO standard 7730 [*37*]. In Case H9, due to the very low heat losses, the floor was not heated, so more thermal stratification developed in the chamber, with higher vertical air temperature differences (Fig. 8). In this case only the requirements for buildings in Category C were achieved.

[place Table 3 approximately here]

[place Table 4 approximately here]

[place Figure 10 approximately here]

4.1.2 Floor cooling

In the case of floor cooling tests, as for floor heating, the vertical air temperature profiles at Point S4 were taken as the reference for occupied zone conditions (Fig . 11).

The data show that the "50%-rule" was never fulfilled in the occupied area and that higher vertical air temperature differences always occurred in the chamber. Analysing the data, it is also evident that increasing the air flow rate, and thus raising the floor temperature, the vertical air temperature differences decreased. This phenomenon is apparent when comparing the vertical air temperature profile in Case C4 (air flow rate 50 l s^{-1}) and Case C6 (air flow rate 80 l s^{-1}) (Fig.12).

The comparison shows that when the floor temperature increases, the vertical air temperature profiles tended to follow the "50%-rule" at several points in the chamber. At Point S4 the temperature profile did not follow the "50%-rule" because the air flow rate of 80 l s^{-1} was probably too high with respect to the

ACCEPTED MANUSCRIPT

chamber dimensions, and thus the air at this point was still too cool. The vertical gradient is nevertheless sensibly reduced from Case C4 to Case C6, even at Point S4 (Tab. 5).

The vertical air temperature differences between head and ankles are generally higher than the limits imposed by ISO standard 7730, due to the action of the floor cooling.

The large vertical gradients probably depend on the fact that with floor cooling the heat transmitted by radiation from the warmer ceiling to the floor is not then transmitted to the supply air at floor level by convection, as was the case in Elisabeth Mundt's experiments [*17, 35*], but it is directly removed by the radiant floor. Under these conditions the temperature of the supply air at floor level does not increase due to convective heat transfer from the floor, as in the case of displacement ventilation and the uncooled floor. Higher vertical air temperature differences therefore occurred.

[place Figure 11 approximately here]

[place Figure 12 approximately here]

[place Table 5 approximately here]

4.2 Air velocity measurements

Air velocity measurements were carried out to verify if draught at ankle level would occur using radiant floor together with displacement ventilation.

Vertical air velocity profiles were derived for all the floor heating and floor cooling cases and an example is given in Fig. 13. Although the calculated Archimedes's number differed, similar air velocity profiles were found in all these cases. The air velocity at 1.10 m at the Point S7 deviated from expectation. By means of smoke tests and CFD analyses *[33]*, it was possible to understand that the air velocity at that point was influenced by the thermal plume due to the manikin's legs and the dummy's legs, in each case rising up from below the table with high turbulence intensity.

The data reported in Fig. 13 reveal the downdraught due to the cooled windows. The air velocity at floor level at Points S1, S2, S3 and S7 was higher than in the occupied zone (S4) and similar to what was found at Points S5 and S6, which were the closest to the supply air terminal device.

Accepted Manuscript

ACCEPTED MANUSCRIPT

Discomfort due to draught may be expressed as the percentage of subjects predicted to find the draught unacceptable. To determine this value, the equation in ISO standard 7730 was used:

$$DR = (34 - T_{a,l}) \cdot (\bar{v}_{a,l} - 0.05)^{0,62} \cdot (0.37 \cdot \bar{v}_{a,l} \cdot Tu + 3.14) \quad (6)$$

As underlined in the standard, this model was derived to predict draught at neck level, so it could overestimate draught at ankle level.

During floor heating tests the draught rate (DR) in the occupied zone (Point S4) was always under 10%, thus under limitations for buildings in Category A (ISO standard 7730). Considering the whole chamber, the draught rate was always below 15%, which is acceptable for buildings in Category B (Tab. 6).

During floor cooling tests draught rate in the occupied zone (Point S4) was always below 15%, which is again acceptable for buildings in Category B. Considering the whole chamber, the draught rate was always below 20%, which is still acceptable for buildings in Category B (Tab. 7).

[place Figure 13 approximately here]

[place Table 6 approximately here]

[place Table 7 approximately here]

4.3 Surface temperature measurements

Surface temperature measurements were used to calculate the mean radiant temperature in the centre of the chamber and in the occupied zone, close to the thermal manikin (Point S4). The operative temperature was then calculated as the adjusted air temperature:

$$T_{op} \approx T_{ad} = \frac{T_a + T_{mr}}{2} \quad (7)$$

Accepted Manuscript

ACCEPTED MANUSCRIPT

The mean radiant temperature in the occupied zone (Point S4), was calculated by using the angle factors between the manikin and the surrounding surfaces (Equation *8*) and the equation reported in ISO standard 7726 [*38*], for the calculation from the plane radiant temperatures (Equation *9*):

$$T_{mr} = \sqrt[4]{\sum_{j=1}^{n} \left(F_{p-j}\ T_j^{\,4}\right)} \tag{8}$$

$$T_{mr} = \frac{0.18 \cdot \left(T_{pr}[up] + T_{pr}[down]\right) + 0.22 \cdot \left(T_{pr}[right] + T_{pr}[left]\right) + 0.30 \cdot \left(T_{pr}[front] + T_{pr}[back]\right)}{2 \cdot \left(0.18 + 0.22 + 0.30\right)} \tag{9}$$

The calculations resulted in similar values, with differences within the accuracy of the probes, so only one value is reported in Tables 8 and 9.

The plane radiant temperatures of the part of the chamber on the left side and on the right side of the manikin were calculated, and used to evaluate the percentage dissatisfied (PD), due to the radiant asymmetry [*39*].

The equations given in ISO standard 7730 were used to calculate the percentage dissatisfied due to the cold wall during floor heating tests and the percentage dissatisfied due to the warm wall during floor cooling tests:

$$PD_{cool\ wall} = \frac{100}{1 + \exp\left(6.61 - 0.345 \cdot \Delta T_{pr}\right)} \tag{10}$$

$$PD_{warm\ wall} = \frac{100}{1 + \exp\left(3.2 - 0.052 \cdot \Delta T_{pr}\right)} - 3.5 \tag{11}$$

These data were compared to the differences in mean equivalent temperature between the left side and the right side of the manikin ($\Delta T_{pr\ manikin}$). This second index provides an indication of the discomfort felt by the occupants and due to radiant asymmetries and draught.

ACCEPTED MANUSCRIPT

The radiant asymmetries calculated by means of the surface temperature measurements (ΔT_{pr}) and the differences of equivalent temperature between the left side and the right side of the manikin ($\Delta T_{pr\ manikin}$), show different values, because the thermal sensation of the manikin depends also on the air temperature and velocity (Tab. 8 and 9). Both of the values are very low. The percentage dissatisfied due to cool or warm walls was always below 1%. No significant radiant asymmetries were thus reported in the room. The percentage dissatisfied due to a cold or warm floor was calculated, using the equation given in ISO standard 7730:

$$PD_{floor} = 100 - 94 \cdot \exp\left(-1.387 + 0.118 \cdot T_{floor} - 0.0025 \cdot T_{floor}^{\ 2}\right) \qquad (12)$$

Very low percentages dissatisfied were found, below 8% for floor heating and below 10% for floor cooling.

[place Table 8 approximately here]

[place Table 9 approximately here]

4.4 Ventilation effectiveness measurements

Ventilation effectiveness was calculated at Points P1 and P2 at heights of 1.10 m, 1.40 m and 1.70 m, in order to evaluate displacement ventilation efficiency in removing contaminants spread by an occupant (simulated by the heated dummy). The results obtained for floor heating and floor cooling are shown in Tables 10 and 11. Values reported for Point P1 are taken as the reference for the occupied zone. During floor heating tests, when the airflow rate was 35 l s^{-1}, the average value of ventilation effectiveness at breathing height (Point P1, 1.10 m) was 1.60, and when the airflow rate was 50 l s^{-1} the average value of ventilation effectiveness at breathing height was 2.00. Displacement ventilation combined with floor heating can thus provide good levels of indoor air quality in the breathing zone. During floor heating tests it was nevertheless not possible to identify a clear contaminant stratification as during floor cooling tests. This situation could be a consequence of the low thermal stratification. Furthermore, careful analysis of Case H9, in which the windows were not cooled, and comparing it to

Accepted Manuscript

ACCEPTED MANUSCRIPT

other cases, reveals that the vertical cooled surfaces had a fundamental influence on contaminant distribution in the chamber (Fig. 14). It was assumed that the cool downdraught took part of the contaminant stratified in the upper part of the chamber and transported it to floor level (CFD analyses confirmed this assumption *[33]*). This is why in Case H2 ventilation effectiveness at 0.85 m had lower value than at 1.10 m. The contaminant at floor level was then transported upwards by the thermal plumes of the heat sources. The fact that some of the contaminant was not properly removed was because of the cooled windows and not because of the floor heating. This phenomenon should be further analysed.

The measurements demonstrated that in the case of contaminant sources linked to heat sources, the spreading of the contaminant can be avoided by using displacement ventilation together with floor heating.

Because of the high values of ventilation effectiveness, it is reasonable to assume that a mixing airflow pattern did not develop. Different results might occur if the contaminant source was located in a different position. However, the situation that was simulated is a typical condition, because displacement ventilation is generally chosen when contaminant sources are also heat sources.

During floor cooling tests, the ventilation effectiveness was always very high: an average value of 2.20 was found when the airflow rate was 50 l s^{-1}, and an average value of 5.70 was found when the airflow rate was 80 l s^{-1}. Lower values were measured in Case H8, because the warmed windows had a higher temperature than in the other cases, and they therefore generated a stronger thermal plume. It was furthermore possible to see a clear decrease in ventilation effectiveness in the upper part of the room, where the contaminant was concentrated.

Displacement ventilation works well when floor cooling is used, because of the marked thermal stratification that occurs.

[place Table 10 approximately here]

[place Table 11 approximately here]

[place Figure 14 approximately here]

Accepted Manuscript

ACCEPTED MANUSCRIPT

4.5 Equivalent temperature measurements

The equivalent temperature of each body part of the thermal manikin was calculated, in order to obtain a detailed description of the local thermal sensations of the occupants.

The equivalent temperature of a body part is the uniform temperature of an imaginary enclosure, with air velocity equal to zero, in which the body part would exchange the same dry heat by radiation and convection as in the actual non-uniform environment. It is thus an expression of the thermal sensation felt by the body part as a result of its heat losses [*31, 32*].

The data obtained in the floor heating tests are summarised in Fig. 15, and should be compared with the air temperatures in Table 8.

The feet and the legs of the manikin indicated lower equivalent temperature values than the other body parts, because of the low temperature of the supply air and the cold downdraught due to the cooled windows. The feet and the legs were nevertheless close to the warm surface of the floor and had a high radiant transfer with it. The floor heating thus reduced the thermal discomfort due to the cool supply air and the downdraught. The difference of equivalent temperature between the feet or the legs and the other body parts was not large.

The thighs, the pelvis and the back showed the highest equivalent temperature values because they were in contact with the chair and thus their heat transfer for convection and radiation with the surroundings was reduced. The thermal insulation of those body parts was greater, due to the thermal insulation of the chair, which is equivalent to an additional layer of clothing.

The left hand indicated higher equivalent temperatures than the right hand because it was very close to the PC casing, with a reduced convective heat transfer with the air and an increased radiant heat transfer with the warm PC. The left forearm and upper arm showed lower equivalent temperatures than the right forearm and upper arm, because they had the highest angle factor to the cold surface of the windows.

In Case H9, when the windows were not cooled, the body parts that were mostly influenced by the radiant heat transfer with them, indicated an increase in the equivalent temperature (Fig. 15). It is especially evident for the left upper arm, the head and the top of the head. The left hand did not show any change during Case H9, because it was shielded form the windows by the PC casing.

Accepted Manuscript

ACCEPTED MANUSCRIPT

When the windows were not cooled, the floor temperature substantially decreased because less heating was required (Tab. 4). The equivalent temperature of the feet and the legs also decreased, because of the reduced temperature of the floor (Fig. 15).

During floor heating measurements, low vertical air temperature differences were found. The air temperature at head height was only 1°C warmer than the air temperature at the feet. The radiant heat transfer between the floor and the feet and between the floor and the legs was much greater than the radiant heat transfer between the floor and the head, which was substantially influenced by other chamber surfaces and especially by cooled windows, as shown by the results of Case H9, when the windows where not cooled. CFD simulations showed that air movements were greater around the head and the top of the head, due to the heat plume *[33]*. The head and the top of the head thus indicated equivalent temperature values similar to those at the feet. The head and the top of the head exchanged heat mainly with cool surfaces while the feet exchanged heat mainly with the warm floor. Higher convective air movements occurred around the head and top of the head with respect to the feet, but the air the at feet was 1°C cooler.

Cases H7 and H8 indicate lower equivalent temperatures than the other cases. In these two tests the operative temperature was lower, because the room set point temperature was lower (Tab. 1 and 8). During these two cases the right thigh did not work properly, because there were electrical contact problems, so these data are not reported.

[place Figure 15 approximately here]

The data obtained in the floor cooling tests are summarised in Fig. 16, and should be compared with the air temperatures reported in Table 9.

During floor cooling tests the floor temperature was lower than the temperature of the surrounding surfaces, and thus it created a cooler radiant environment at the feet. The increased thermal stratification also gave rise to a warmer environment in the upper part of the chamber and a cooler environment at floor level.

These phenomena explain why, during floor cooling tests, the difference of equivalent temperature between the feet or the legs and the other body parts was higher than during floor heating tests. The feet

Accepted Manuscript

ACCEPTED MANUSCRIPT

and the legs indicated the lowest equivalent temperature in the chamber. The thighs, the pelvis and the back again indicated the highest equivalent temperature because they were in contact with the chair. The right hand indicated high values of equivalent temperature because of the high radiant heat exchange with the desk light. The right upper arm, with a reduced clothing insulation during floor cooling tests, had a higher convective heat transfer, because airflow rates were higher than in the floor heating tests. The top of the head indicated lower equivalent temperatures than the head because it had a higher angle factor with the cool floor and it was more exposed to convective air movements. The section designated "top of the head" consists of the scull and the back of the neck, which during floor cooling tests was not protected by any clothing, because the manikin was wearing a T-shirt. The head (i.e., the face) of the manikin was shielded from the floor by the desk and the PC, which had warmer surface temperatures than the floor.

An influence of the warm windows was detected in Cases C8 and C9, when their temperature was increased up to 37°C. During these two cases the equivalent temperature of the head and of the top of the head increased slightly.

In summary, the thermal manikin did not indicate any particular problems of local thermal discomfort due to radiation or convection, either during floor heating tests or during floor cooling tests. Only the cold windows, in the floor heating tests, generated any appreciable radiant asymmetry.

In accordance with previous research by Cheong et al. [*40*] the measurements show that variations of temperature between body parts for different thermal gradients, at a given room air temperature, are almost the same, and the variation decreases when room temperature increases. During floor cooling measurements, the manikin indicated lower temperature differences between body parts than during floor heating measurements.

[place Figure 16 approximately here]

5. Discussion

Accepted Manuscript

ACCEPTED MANUSCRIPT

The measurements and the results reported in this paper focus on thermal comfort and ventilation effectiveness aspects of the combination of radiant floor heating or cooling with displacement ventilation. The potential and the limitations related to the use of the hybrid system have been highlighted, although further studies focused on energy effectiveness will be required to provide a complete description of the issue.

If floor heating is combined with displacement ventilation, the air can be supplied at a lower temperature, which can extend the free running period (no pre-heating) for the ventilation system, depending on the external climate, with a resulting reduction in the energy consumption.

Floor cooling alone is able to cover up to 50 W/m^2 [1], and in buildings with normal cooling loads it can substantially reduce the cooling effect required for displacement ventilation. By using high temperature heat sources (13-20°C) [28-41], floor cooling can help reducing the energy consumption of the system.

Further detailed measurements and analyses should be performed to confirm the general observations made above, and these should also consider the effect of relative humidity.

6. Conclusions

The measurements reported in this paper indicate that under the simulated boundary conditions, all of which occur widely in practice, floor heating can be combined with displacement ventilation in an office room, maintaining high values of ventilation effectiveness.

The “50% rule” can no longer be used to determine the vertical air temperature gradient in a room when a radiant floor is used together with displacement ventilation. New methods of calculating this value are proposed, using an “80%-rule” as the limit for a floor heating capacity of about 60 W m^{-2}.

The ventilation effectiveness measurements confirmed that contaminant concentration at the breathing height (1.10 m) in the occupied zone was always lower than contaminant concentration in the upper part of the chamber and in the exhaust. This indicates that, if occupants are the main contaminant sources inside the room, displacement ventilation will guarantee high levels of indoor air quality, even when combined with radiant floor heating. Further measurements are needed to evaluate ventilation effectiveness in cases where there are other contaminant sources.

Accepted Manuscript

ACCEPTED MANUSCRIPT

The downdraught due to the cooled windows substantially affected contaminant distribution. Particular attention should be paid in the design phase to avoid locating contaminant sources close to cold vertical surfaces if a displacement ventilation system is used. Further measurements on the influence of cold vertical surfaces on ventilation effectiveness are required.

The measurements showed also that the use of floor cooling combined with displacement ventilation does not increase the draught risk at ankle level, *under the simulated boundary conditions and thus within the maximum room cooling load of 76 W m^{-2}*. The vertical air temperature differences between head and ankles were outside the comfort range suggested by the standards, because floor cooling reduced the effect of radiant heat transfer between the warm ceiling and the floor, and thus the supply air at floor level was not warmed convectively by the floor, so its temperature remained unchanged.

This phenomenon is probably less important in buildings with tall ceilings where floor cooling is generally used, and in buildings with high solar loads. In these buildings, lower vertical air temperature differences occur, and thus the use of floor cooling should not create any local thermal discomfort. Further measurements are required to verify this conclusion.

The results obtained using the thermal manikin showed the presence of thermal stratification in the room. The vertical temperature differences between the head and the ankles were moderate.

7. Nomenclature

c_e	Contaminant concentration in the exhaust	kg/kg
c_j	Contaminant concentration at the measured point	kg/kg
c_s	Contaminant concentration in the supply air	kg/kg
DR	Draught rate	%
$F_{p\text{-}j}$	Angle factor between person and j-surface	–
H	Chamber net height	m
h_j	Heat transfer coefficient of the body part	W m^{-2} K^{-1}
k	Dimensionless temperature of the air near the floor	-
PD	Percentage dissatisfied	%
Q_h	*Floor heating capacity*	*W m^{-2}*

ACCEPTED MANUSCRIPT

Q_i	Internal heat gains	W
Q_j	Heat loss of the body part	W m^{-2}
q_v	Ventilation flow rate	l s^{-1}
T_a	Air temperature	°C
$T_{a,l}$	Local air temperature	°C
T_{ad}	Adjusted air temperature	°C
T_e	Exhaust air temperature	°C
T_{eq}	Equivalent temperature	°C
T_f	Temperature of the air near the floor	°C
T_{floor}	Floor temperature	°C
T_j	Surface temperature	K
T_{mr}	Mean radiant temperature	°C
T_{op}	Operative temperature	°C
T_{pr}	Plane radiant temperatures	°C
T_r	*Set-point room air temperature (measured at the room centre, 1.1 m above the floor level)*	°C
T_{sk}	Skin temperature	°C
T_s	Supply air temperature	°C
T_w	Heated/cooled windows surface temperature	°C
T_y	Air temperature at height y	°C
Tu	Turbulence intensity	%
y	Height of measurement	m
$\bar{v}_{a,l}$	Local mean air velocity	m/s
$\Delta T_{0.1\text{-}1.1}$	Vertical air temperature difference between head and ankles	°C
ΔT_{pr}	Radiant asymmetry	°C
$\Delta T_{pr\ manikin}$	Temperature difference between left and right side of the manikin	°C
ε	Ventilation effectiveness	–

Accepted Manuscript

ACCEPTED MANUSCRIPT

Acknowledgments

This work was part of a research program on radiant floor performances funded by Velta-Italia.

The authors wish to thank Professor Arsen K. Melikov for his valuable advice and help.

References

[1] B.W. Olesen, Possibilities and limitations of radiant floor cooling, ASHRAE Transactions 103 vol. 1 (1997) 42–48

[2] B.W. Olesen, Radiant floor heating in theory and practice, ASHRAE Journal 7 (2002) 19–24

[3] P. Simmonds, S. Holst, S. Reuss, W. Gaw, Comfort conditioning for large spaces, ASHRAE Transactions 105 vol. 1 (1999) 1037–1048

[4] E. Baskin, Project 4.3: Residential radiant cooling and heating assessment, Oak Ridge National Laboratory, Oak Ridge, Tennessee, 31 March 2003

[5] J. Niu, J.v.d. Kooi, 2-dimensional simulation of air-flow and thermal comfort in a room with open-window and indoor cooling systems, Energy and Buildings 18 (1992) 65–75

[6] J. Niu, J.v.d. Kooi, Indoor climate in rooms with cooled ceiling systems, Building and Environment 29 (1994) 283–290

[7] C. Stetiu, H.E. Feustel, F.C. Winkelmann, Development of a model to simulate the performance of hydronic radiant cooling ceilings, ASHRAE Transactions 101 vol.2 (1995) 730–743

[8] H.E. Feustel, C. Stetiu, Hydronic radiant cooling - preliminary assessment, Energy and Buildings 22 (1995) 193–205

[9] J. Niu, J.v.d. Kooi, H.v.d. Ree, Energy saving possibilities with cooled-ceiling systems, Energy and Buildings 23 (1995) 147–158

[10] C. Stetiu, Energy and peak power savings potential of radiant cooling systems in US commercial buildings, Energy and Buildings 30 (1999) 127–138

[11] J. Miriel, L. Serres, A. Trombe,, Radiant ceiling panel heating–cooling systems: experimental and simulated study of the performances, thermal comfort and energy consumptions, Applied Thermal Engineering 22 (2002) 1861–1873

Accepted Manuscript

ACCEPTED MANUSCRIPT

[12] S. Sattari, B. Farhanieh, A parametric study on radiant floor heating system performance, Renewable Energy 31 (2006) 1617–1626

[13] B.W. Olesen, L. Mattarolo, Thermal comfort and energy performance of hydronic radiant cooling systems compared to convective systems, in: Proceeding of Healthy Buildings 2009, Syracuse (NY), 13-17 September 2009

[14] E. Fabrizio, S. P. Corgnati, F. Causone, M. Filippi, L. Schiavio, Contrasting the energy and comfort performance of radiant heating and cooling system vs. all air systems by numerical simulation, in: Proceeding of CLIMA 2010 Sustainable Energy Use in Buildings, Antalya, 9-12 May 2010

[15] B.W. Olesen, F. Bonnefoi, E. Michel, M. De Carli, Heat exchange coefficient between floor surface and space by floor cooling - Theory or a question of definition, ASHRAE Transactions: Symposia DA-00-8-2 (2000) 684–694

[*16*] H. Skistad, E. Mundt, P.V. Nielsen, K. Hagstrom, J. Ralio, Displacement ventilation in non-industrial premises, Rehva, Brussels, 2002

[*17*] E. Mundt, The performance of displacement ventilation system – Experimental and theoretical studies, Ph.d Thesis, Bulletin n.38, Building Services Engineering, KTH, Stockholm, 1996

[*18*] T. Abbas, Code of practice 17/99: Displacement ventilation and static cooling devices, BSRIA, Bracknell, 1999

[*19*] European Committee for Standardization, CEN Report 1752: Ventilation for buildings - design criteria for the indoor environment, CEN, Brussels, 1998

[*20*] K. Fitzner, Displacement ventilation and cooled ceilings, results of laboratory tests and practical installations, in: Proceedings of Indoor Air 96, Nagoya, Japan, 21-26 July 1996

[*21*] S.C. Carpenter, J.P. Kokko, Radiant heating and cooling, displacement ventilation with recovery and storm water cooling: an environmentally responsible HVAC system, ASHRAE Transactions 104 vol. 2 (1998) 1321–1326

[*22*] M. Behne, Indoor air quality in rooms with cooled ceilings. Mixing ventilation or rather displacement ventilation?, Energy and Buildings 30 (1999) 155–166

[*23*] J-W. Jeong, S.A. Mumma, W.P. Bahnfleth, Energy conservation benefits of a dedicated outdoor air system with parallel sensible cooling by ceiling radiant panels, ASHRAE Transactions 109 vol. 2 (2003) 627–636

Accepted Manuscript

ACCEPTED MANUSCRIPT

[*24*] X. Hao, G. Zhang, Y. Chen, S. Zou, D.J. Moschandreas, A combined system of chilled ceiling, displacement ventilation and desiccant dehumidification, Building and Environment 42 (2007) 3298–3308

[*25*] H. Skistad, Floor heating and displacement ventilation, in: Proceedings of Cold Climate HVAC 2003, Trondheim, 15-18 June 2003

[26] Y. Ren, D. Li, Y. Zhang, Experimental Study of the Floor Radiant Cooling System Combined with Displacement Ventilation, in: Proceeding of ICEBO 2006, Shenzhen, China

[*27*] W. Kessling, S. Holst, M. Schuler, Innovative design concept for the new Bangkok international airport, NBI**A**, Symposium on Improving Building Systems in Hot and Humid Climates, Richardson, 17-19 May 2004

[*28*] J. Babiak, B.W. Olesen, D. Petras, Low temperature heating and high temperature cooling, Rehva, Brussels, 2007

[*29*] J. Toftum, G. Langkilde, P.O. Fanger, New indoor environment chambers and field experiment offices for research on human comfort, health and productivity at moderate energy expenditure, Energy and Buildings 36 (2004) 899–903

[*30*] S. Tanabe, E.A. Arens, F.S. Bauman, H. Zhang, T.L. Madsen, Evaluating thermal environments by using a thermal manikin with controlled skin surface temperature, ASHRAE Transactions 100 vol. 1 (1994) 39–48

[*31*] H. Nilsson, I. Holmer, M. Bohm, O. Noren, Definition and theoretical background of the equivalent temperature, in: Proceedings of CABCLI seminar, Firenze, 18-19 November 1999

[*32*] A. Melikov, H. Zhou, Comparison of methods for determining t_{eq} under well-defined conditions, in: Proceedings of CABCLI seminar, Firenze, 18-19 November 1999

[33] F. Causone, B.W. Olesen, S.P. Corgnati, Floor heating with displacement ventilation: an experimental and numerical analysis, HVAC&R Research 16 (2) 2010, 139–160

[*34*] EN 15251: 2007 - Ventilation for buildings – Indoor environmental input parameters for design and assessment of energy performance of buildings addressing indoor air quality, thermal environment, lighting and acoustics

[*35*] E. Mundt, Displacement ventilation systems – convection flows and temperature gradients, Building and Environment 30 (1995) 129–133

Accepted Manuscript

ACCEPTED MANUSCRIPT

[36]H. Skistad, Displacement Ventilation, Research Studies Press Ldt, Somerset, 1994

[*37*] ISO 7730: 2005 - Ergonomics of the thermal environment - Analytical determination and interpretation of thermal comfort using calculation of the PMV and PPD indices and local thermal comfort criteria

[*38*] ISO 7726: 1998 - Ergonomics of the thermal environment - Instruments for measuring physical quantities

[*39*] P.O. Fanger, B.M. Ipsen, G. Langkilde, B.W. Olesen, N.K. Christensen, S. Tanabe, Comfort limits for asymmetric thermal radiation, Energy and Buildings 8 (1985) 225–236

[*40*] K.W.D. Cheong, W.J. Yu, R. Kosonen, K.W. Tham, S.C. Sekhar, Assessment of thermal environment using a thermal manikin in a field environment chamber served by displacement ventilation system, Building and environment 41 (2006) 1661–1670

[41] F. Causone, S.P. Corgnati, E. Fabrizio, M. Filippi, Radiant Systems, Uponor Technical Guideline, 2009

Accepted Manuscript

ACCEPTED MANUSCRIPT

Figure 1. The indoor environment chamber

Figure 2. The experimental equipment

Figure 3. The seven points where air temperature and velocity profiles were taken (S1-S7) and the position of the probes on the unheated walls A and B

Figure 4. Position of the probes on the ceiling and on the wall where the supply air terminal device was located

Figure 5. Position of the probes on the floor and on the heated/cooled windows

Figure 6. The points where contaminant concentration measurements were taken

Figure 7. Correlation between the dimensionless temperature of the air at floor level and the temperature difference between the floor surface and the operative temperature in the room

Figure 8. The dimensionless vertical air temperature profiles in the occupied zone do not follow the "50%-rule" when floor heating is used

Figure 9. Correlation between the temperature profile in the occupied zone and the floor heating capacity

Figure 10. Example of vertical air temperature profiles in different positions inside the chamber during a floor heating test (H1)

Figure 11. Dimensionless vertical air temperature profiles in the occupied zone during floor cooling tests

Accepted Manuscript

ACCEPTED MANUSCRIPT

Figure 12. Comparison of vertical air temperature profiles between Case C4 (airflow rate 50 l s^{-1}) and Case C6 (airflow rate 80 l s^{-1})

Figure 13. Example of vertical air velocity profiles during floor heating measurements

Figure 14. Comparison between ventilation effectiveness when windows were cooled (up; H2) and when they were not cooled (down; H9)

Figure 15. Equivalent temperature of the body parts during floor heating measurements

Figure 16. Equivalent temperature of the body parts during floor cooling measurements

Accepted Manuscript

ACCEPTED MANUSCRIPT

Accepted Manuscript

Table 1

		H1	H2	H3	H4	H5	H6	H7	H8	H9
T_r	°C	22.0	22.0	22.0	22.0	22.0	22.0	20.0	20.0	22.0
T_w	°C	13.5	13.5	13.5	13.5	13.5	13.5	12.0	12.0	-
T_s	°C	14.0	16.0	18.0	14.0	16.0	18.0	16.0	16.0	14.0
q_v	$l\ s^{-1}$	35.0	35.0	35.0	50.0	50.0	50.0	35.0	50.0	35.0
	h^{-1}	3.1	3.1	3.1	4.5	4.5	4.5	3.1	4.5	3.1
Q_i	W	520	520	520	520	520	520	520	520	520
	$W\ m^{-2}{}_{floor}$	31.0	31.0	31.0	31.0	31.0	31.0	31.0	31.0	31.0

Accepted Manuscript

Table 2

		C1	C2	C3	C4	C5	C6	C7	C8	C9	C10
T_r	°C	26.0	26.0	26.0	26.0	26.0	26.0	26.0	26.0	26.0	26.0
T_w	°C	33.2	33.2	33.2	33.2	33.2	33.2	33.2	37.1	37.1	-
T_s	°C	16.0	16.0	18.0	20.0	18.0	20.0	22.0	20.0	22.0	20.0
q_v	$l\ s^{-1}$	35.0	50.0	50.0	50.0	80.0	80.0	80.0	80.0	80.0	50.0
	h^{-1}	3.1	4.5	4.5	4.5	7.1	7.1	7.1	7.1	7.1	4.5
Q_i	W	520	520	520	520	520	520	520	520	520	520
	$W\ m^{-2}_{floor}$	31.0	31.0	31.0	31.0	31.0	31.0	31.0	31.0	31.0	31.0

Accepted Manuscript

Table 3

	H1	H2	H3	H4	H5	H6	H7	H8	H9
S1	0.5	0.5	0.2	0.6	0.5	0.2	0.1	0.4	0.6
S2	0.7	0.6	0.4	0.7	0.8	0.5	0.3	0.7	0.6
S3	0.6	0.5	0.3	0.8	0.6	0.4	0.3	0.5	0.6
S4	0.8	0.8	0.7	0.8	0.8	0.8	0.5	0.6	0.5
S5	0.6	0.6	0.5	0.6	0.6	0.6	0.4	0.5	0.4
S6	0.6	0.5	0.5	0.5	0.5	0.4	0.4	0.4	0.4
S7	0.5	0.5	0.2	0.6	0.5	0.2	0.2	0.4	0.6

Accepted Manuscript

Table 4

	H1	H2	H3	H4	H5	H6	H7	H8	H9
$\Delta T_{0.1\text{-}1.1}$	0.9	0.4	0.5	1.2	1.1	0.5	0.8	0.9	3.8
T_{floor}-T_{op}	4.9	4.3	3.5	5.7	5.0	4.0	1.5	3.1	no heating
T_{floor}	27.2	26.1	25.2	27.8	27.2	25.8	21.0	23.6	21.5
Q_h	54	47	39	62	55	44	16	34	no heating

Accepted Manuscript

Table 5

	C1	C2	C3	C4	C5	C6	C7	C8	C9	C10
$\Delta T_{0.1\text{-}1.1}$	6.6	6.1	5.8	5.6	4.6	3.9	3.6	5.2	5.3	3.2
$T_{floor} - T_{op}$	-5.2	-4.0	-5.0	-6.1	-1.7	-2.8	-5.3	-7.1	-7.8	-1.3
T_{floor}	20.8	22.1	20.8	19.4	24.7	23.4	20.7	19.2	18.7	24.3

Accepted Manuscript

Table 6

	H1	H2	H3	H4	H5	H6	H7	H8	H9
S1	12	12	12	11	11	11	7	9	5
S2	9	10	10	10	10	10	7	8	4
S3	10	11	11	10	11	11	12	8	0
S4	6	5	5	9	9	6	6	9	4
S5	7	5	5	9	8	6	4	8	5
S6	7	6	6	10	9	8	6	10	5
S7	14	14	14	12	13	15	13	13	0

Accepted Manuscript

Table 7

	C1	C2	C3	C4	C5	C6	C7	C8	C9	C10
S1	0	3	0	4	3	2	3	4	5	1
S2	0	1	0	4	5	4	4	4	5	0
S3	0	0	0	0	5	4	3	3	3	0
S4	4	7	8	3	14	13	12	13	12	6
S5	5	6	5	5	11	9	9	12	10	4
S6	5	9	9	9	14	13	14	17	16	7
S7	0	1	0	1	3	0	0	0	0	0

Accepted Manuscript

Table 8

		H1	H2	H3	H4	H5	H6	H7	H8	H9
centre of the chamber	$T_{a\,1.10}$ [°C]	22.3	21.8	21.7	22.0	22.1	21.8	19.6	20.5	23.5
	T_{mr} [°C]	22.3	21.8	21.6	22.3	22.3	21.8	19.5	20.6	22.7
	T_{op} [°C]	22.3	21.8	21.7	22.1	22.2	21.8	19.5	20.5	23.1
point S4	$T_{a\,1.10}$ [°C]	22.0	21.6	21.5	21.8	21.9	21.6	19.5	20.3	23.6
	T_{mr} [°C]	22.2	21.6	21.3	22.3	22.1	21.6	19.0	20.4	22.5
	T_{op} [°C]	22.1	21.6	21.4	22.1	22.0	21.6	19.3	20.3	23.0
	ΔT_{pr} [°C]	3.8	3.6	3.6	3.6	3.6	3.6	2.4	2.8	0.4
	$\Delta T_{pr\,manikin}$ [°C]	0.1	0.1	0.2	0.1	0.0	0.1	1.2	0.6	0.4
	$PD_{cool\,wall}$ [%]	0.5	0.5	0.5	0.5	0.5	0.5	0.3	0.4	0.2
	$PD_{warm\,floor}$ [%]	7.1	6.1	5.7	7.8	7.1	6.0	7.8	5.6	6.8

Table 9

		C1	C2	C3	C4	C5	C6	C7	C8	C9	C10
centre of the chamber	$T_{a\,1.10}$ [°C]	26.6	26.3	26.2	26.0	26.1	26.1	26.1	26.3	26.5	25.7
	T_{mr} [°C]	25.5	25.8	25.4	25.0	26.7	26.4	25.8	26.3	26.4	25.4
	T_{op} [°C]	26.0	26.1	25.8	25.5	26.4	26.2	26.0	26.3	26.5	25.6
point S4	$T_{a\,1.10}$ [°C]	27.1	26.7	26.6	26.5	26.5	26.4	26.4	26.5	27.1	25.9
	T_{mr} [°C]	25.4	25.8	25.3	24.7	27.0	26.5	25.6	26.2	26.1	25.2
	T_{op} [°C]	26.3	26.3	25.9	25.6	26.8	26.4	26.0	26.3	26.6	25.6
	ΔT_{pr} [°C]	3.0	2.9	3.0	3.1	2.8	2.7	2.8	4.6	4.7	0.4
	$\Delta T_{pr\ ranking}$ [°C]	0.7	0.8	0.8	0.8	0.8	0.8	0.8	1.0	1.0	0.5
	PD $_{warm\ wall}$ [%]	0.0	0.0	0.0	0.0	0.0	0.0	0.0	0.0	0.0	0.0
	PD $_{cool\ floor}$ [%]	7.4	6.1	7.3	9.3	5.7	5.5	7.2	9.5	10.1	5.5

Manuscript

Table 10

		H1	H2	H3	H4	H5	H6	H7	H8	H9
P1	0.60 m	-	1.26	-	-	-	-	-	-	20.58
	0.85 m	-	1.41	-	-	-	-	-	-	-
	1.10 m	1.63	1.55	1.42	2.00	2.00	1.79	2.07	2.52	1.50
	1.40 m	1.62	1.32	1.26	1.89	2.13	1.61	1.48	2.02	1.59
	1.70 m	1.34	1.23	1.13	1.71	1.69	1.40	1.31	1.82	1.57
P2	0.60 m	-	1.44	-	-	-	-	-	-	15.61
	0.85 m	-	1.62	-	-	-	-	-	-	-
	1.10 m	1.90	1.55	1.63	2.14	2.14	1.72	2.07	2.20	1.69
	1.40 m	1.92	1.36	1.48	2.60	2.72	1.93	1.31	2.28	1.61
	1.70 m	1.38	1.14	1.24	1.81	1.77	1.35	1.36	1.57	1.53

Table 11

		C1	C2	C3	C4	C5	C6	C7	C8	C9	C10
P1	0.60 m	-	-	-	-	-	-	-	-	-	-
	0.85 m	1.14	-	-	-	-	10.3	-	8.59	6.61	
	1.10 m	1.15	2.75	2.14	1.73	5.76	8.38	4.64	4.21	2.11	2.44
	1.40 m	1.18	1.04	1.13	1.13	1.25	0.98	1.83	1.01	0.92	4.48
	1.70 m	1.07	1.13	0.98	1.09	0.81	0.78	0.75	0.94	0.82	2.81
P2	0.60 m	-	-	-	-	-	-	-	-	-	-
	0.85 m	1.17	-	-	-	-	12.19	-	3.32	3.47	-
	1.10 m	1.13	1.23	1.22	1.13	2.49	2.64	1.66	0.89	0.97	2.63
	1.40 m	0.97	0.79	0.77	0.91	0.78	0.68	0.86	0.78	0.78	2.30
	1.70 m	1.00	0.77	0.60	0.81	0.48	0.41	0.80	0.85	0.82	1.90

Manuscript

Figure 1

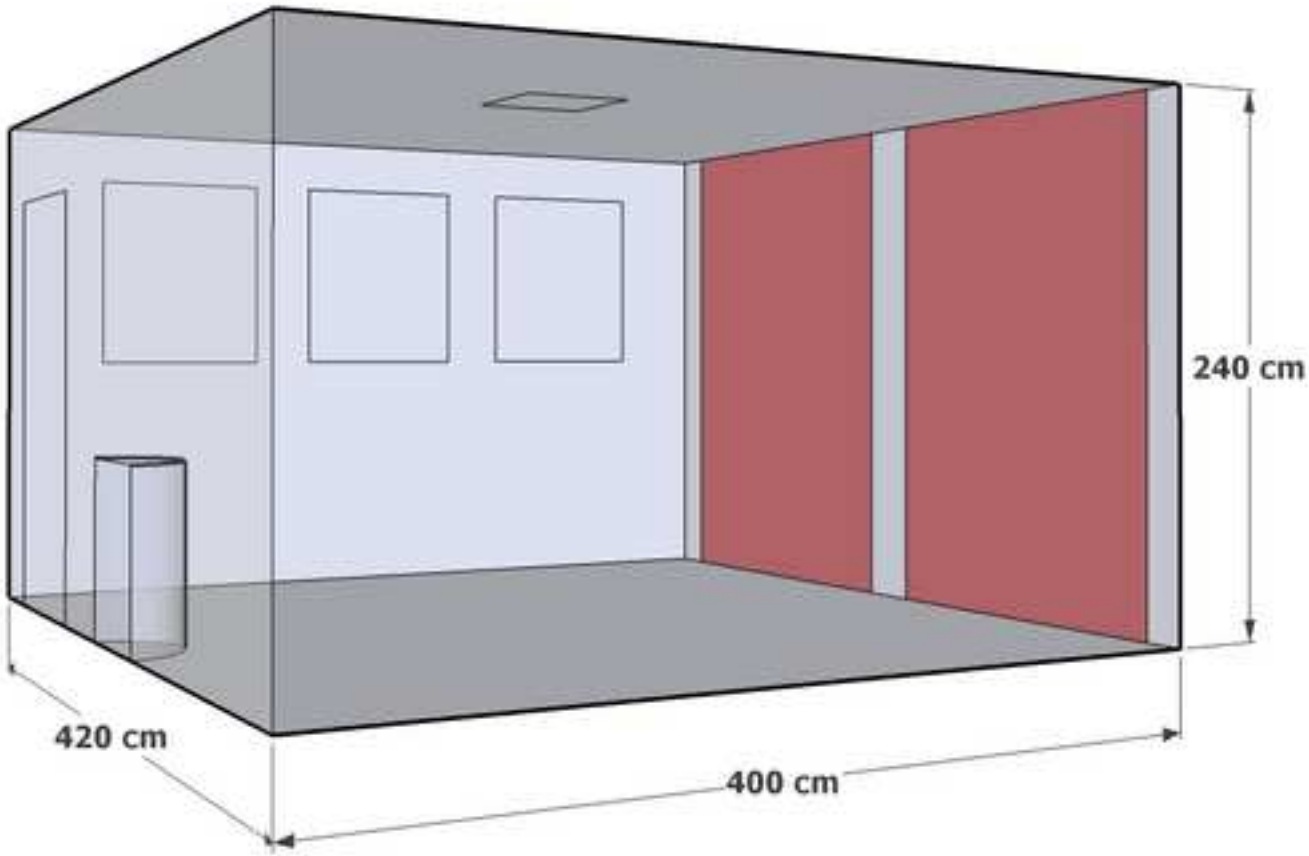

Figure 2

Figure 3

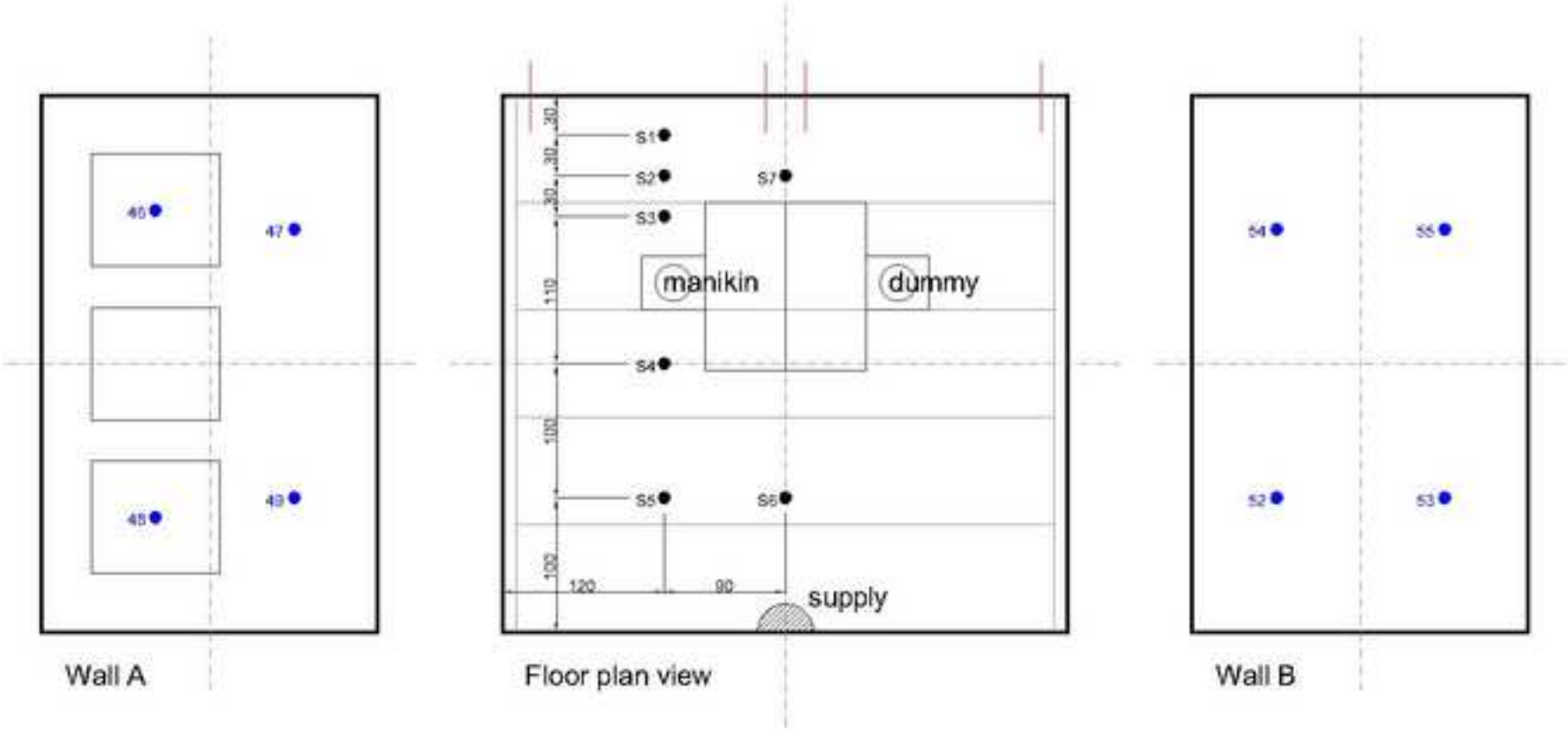
46
47
48
49
Wall A
S1
S2
S3
S4
S5
S6
S7
manikin
dummy
120
90
supply
Floor plan view
54
55
52
53
Wall B

Figure 4

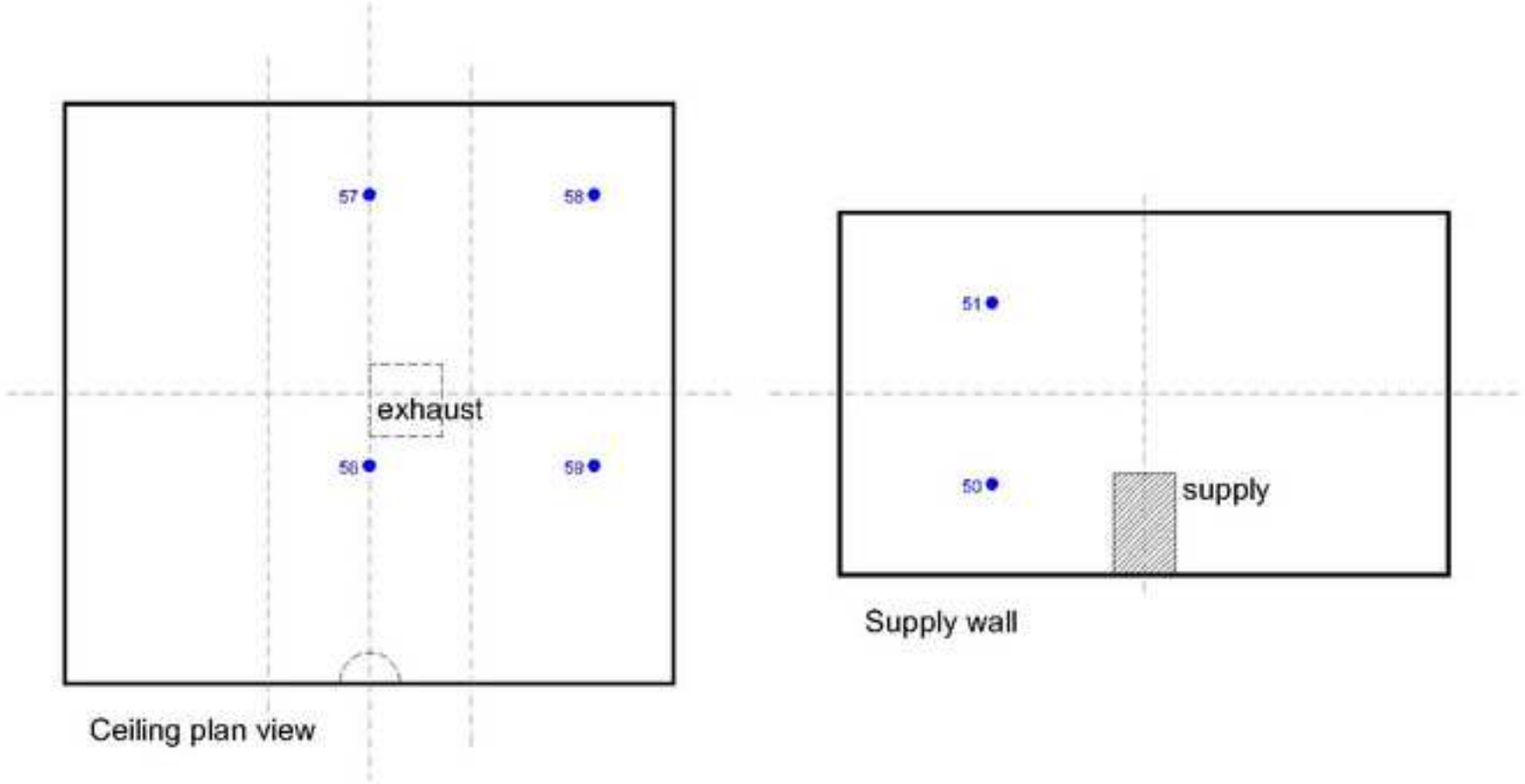
57
58
exhaust
56
59
Ceiling plan view
51
50
supply
Supply wall

Figure 5

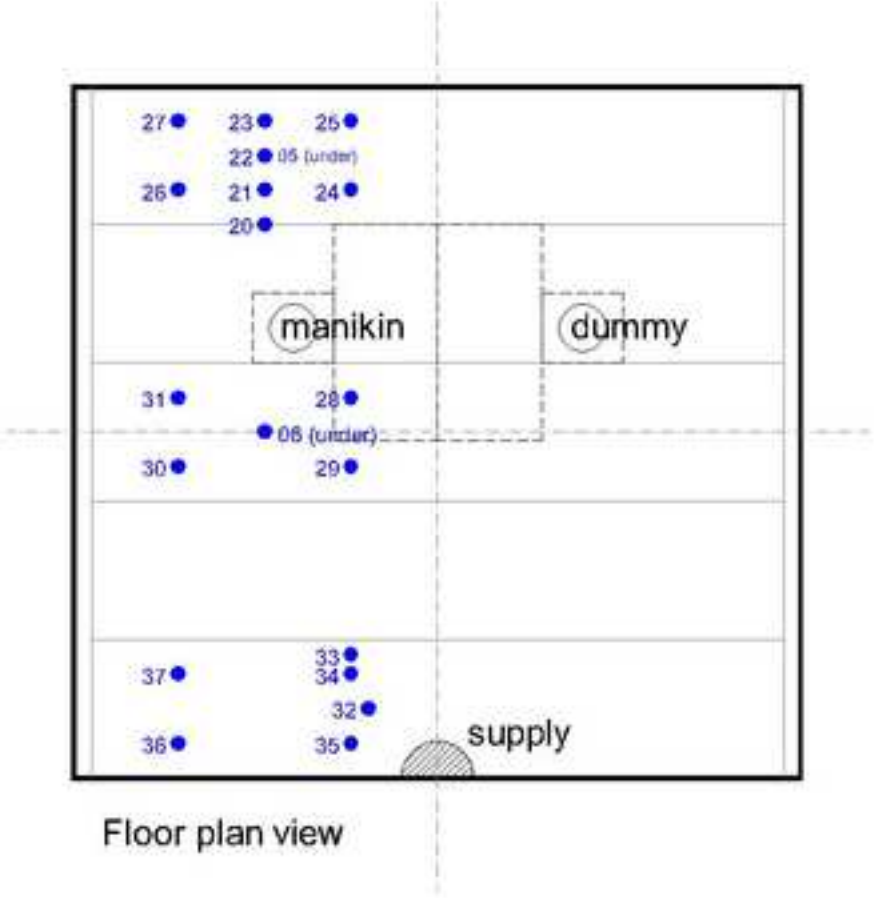

Floor plan view

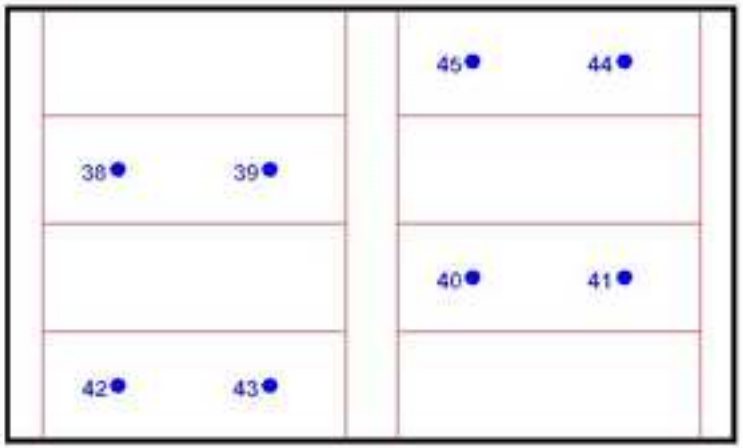

Heating/cooling plastic plates (red panels)

ACCEPTED MANUSCRIPT

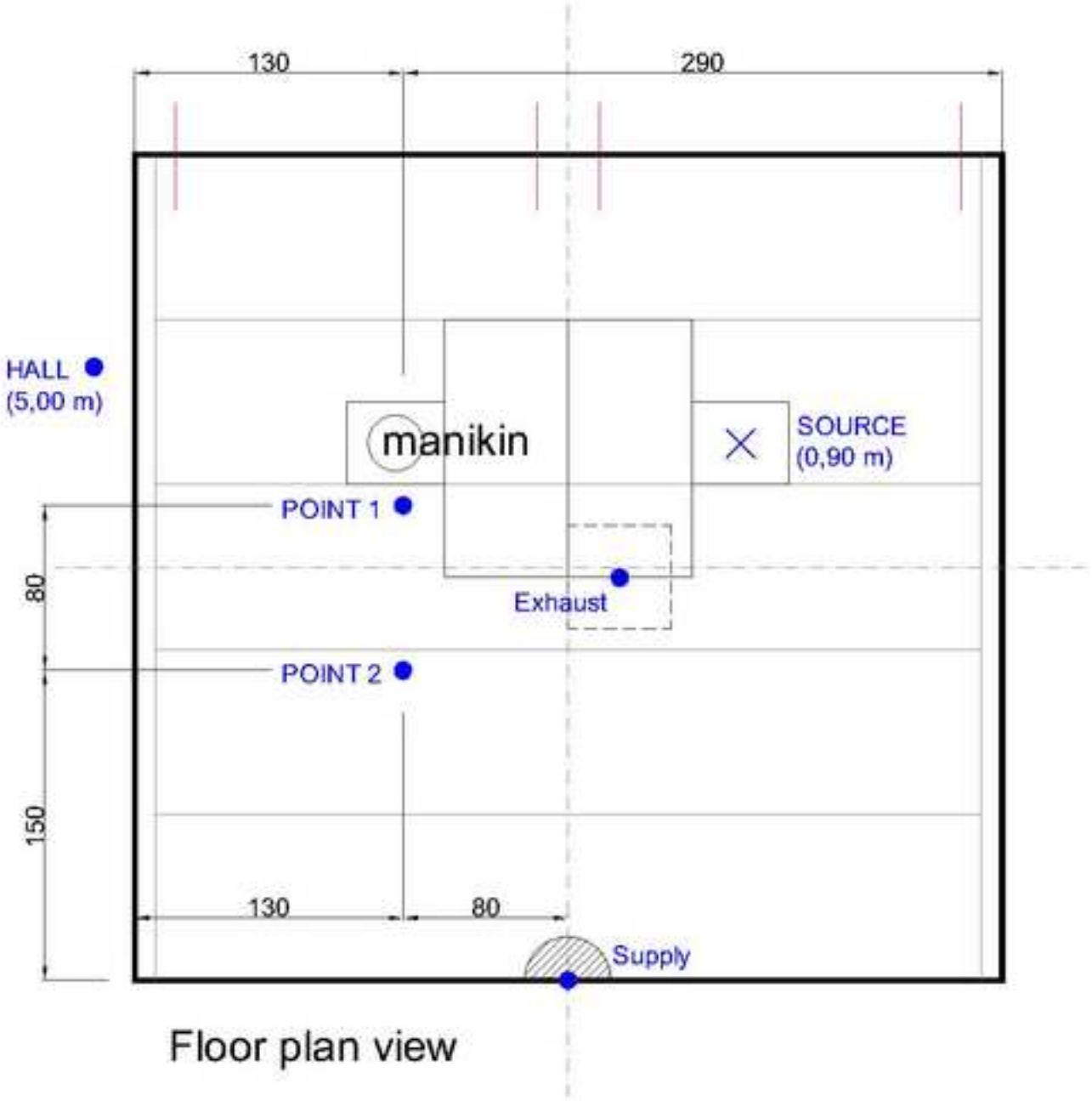

Floor plan view

Figure 7

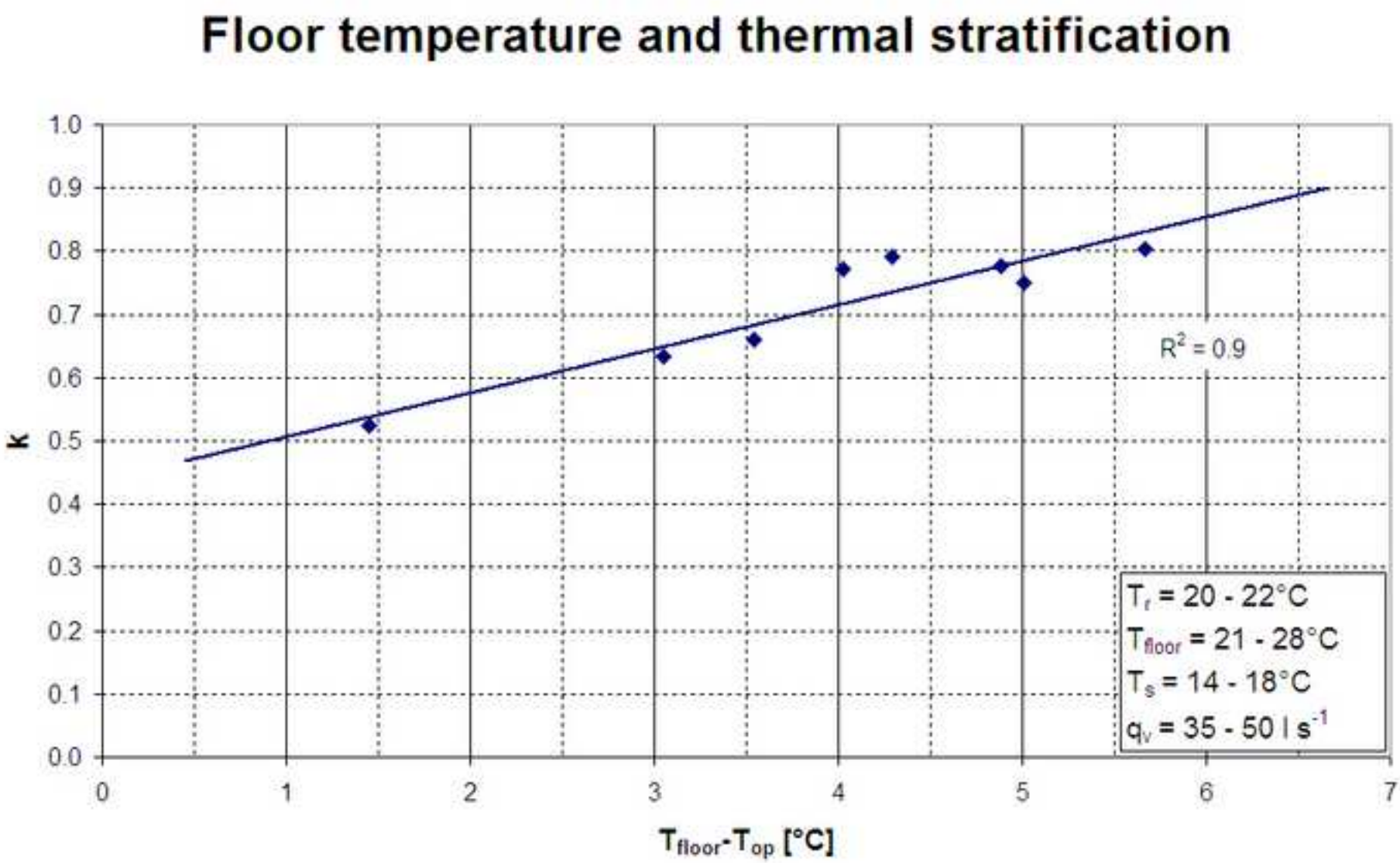
Floor temperature and thermal stratification
1.0
0.9
0.8
0.7
0.6
0.5
0.4
0.3
0.2
0.1
0.0
k
0
1
2
3
4
5
6
7
T_{floor}-T_{op} [°C]
R^2 = 0.9
T_r = 20 - 22°C
T_{floor} = 21 - 28°C
T_s = 14 - 18°C
q_v = 35 - 50 l s^{-1}

Figure 8

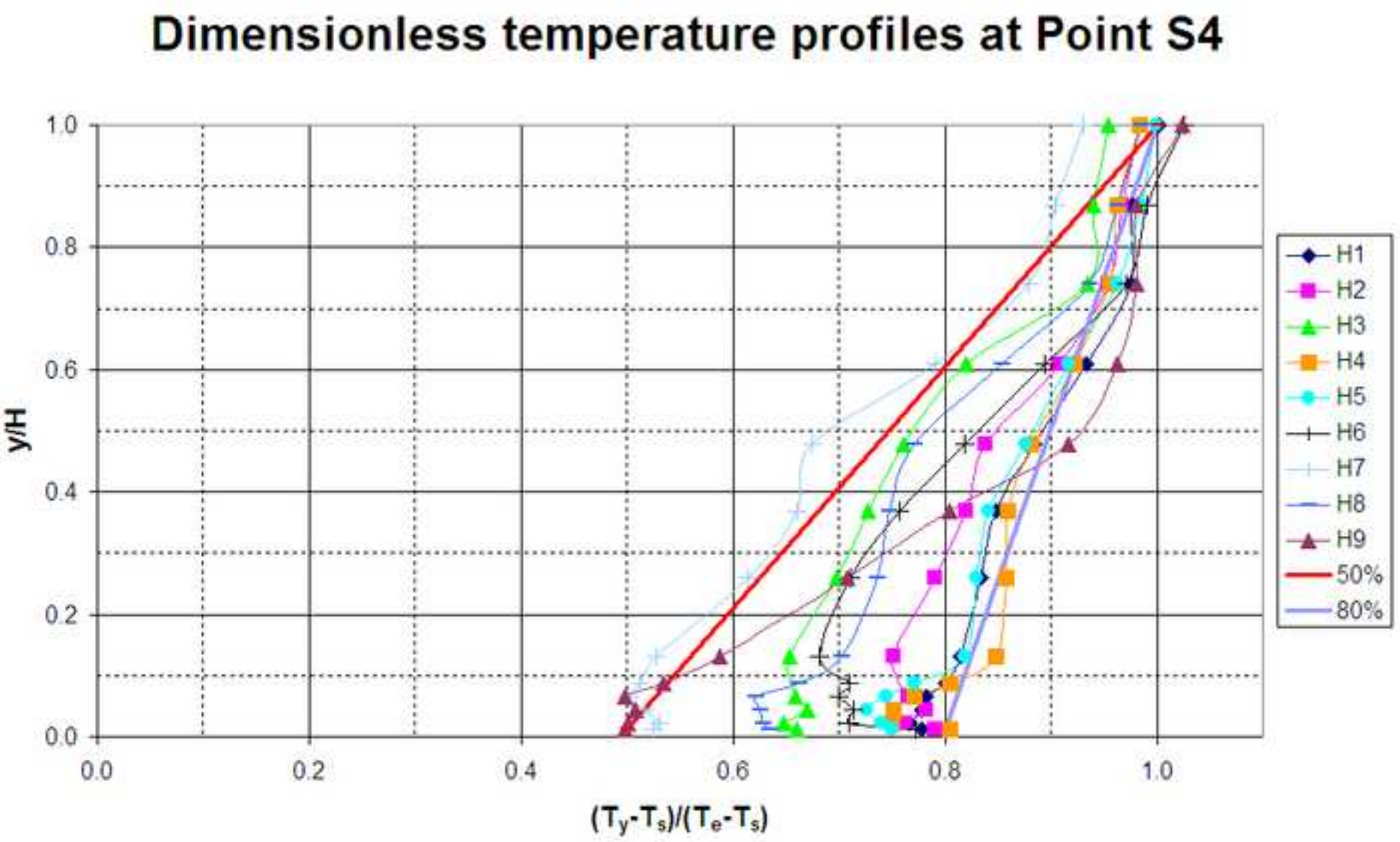
Dimensionless temperature profiles at Point S4
y/H
1.0
0.8
0.6
0.4
0.2
0.0
0.0
0.2
0.4
0.6
0.8
1.0
(Ty-Ts)/(Te-Ts)
H1
H2
H3
H4
H5
H6
H7
H8
H9
50%
80%

Figure 9

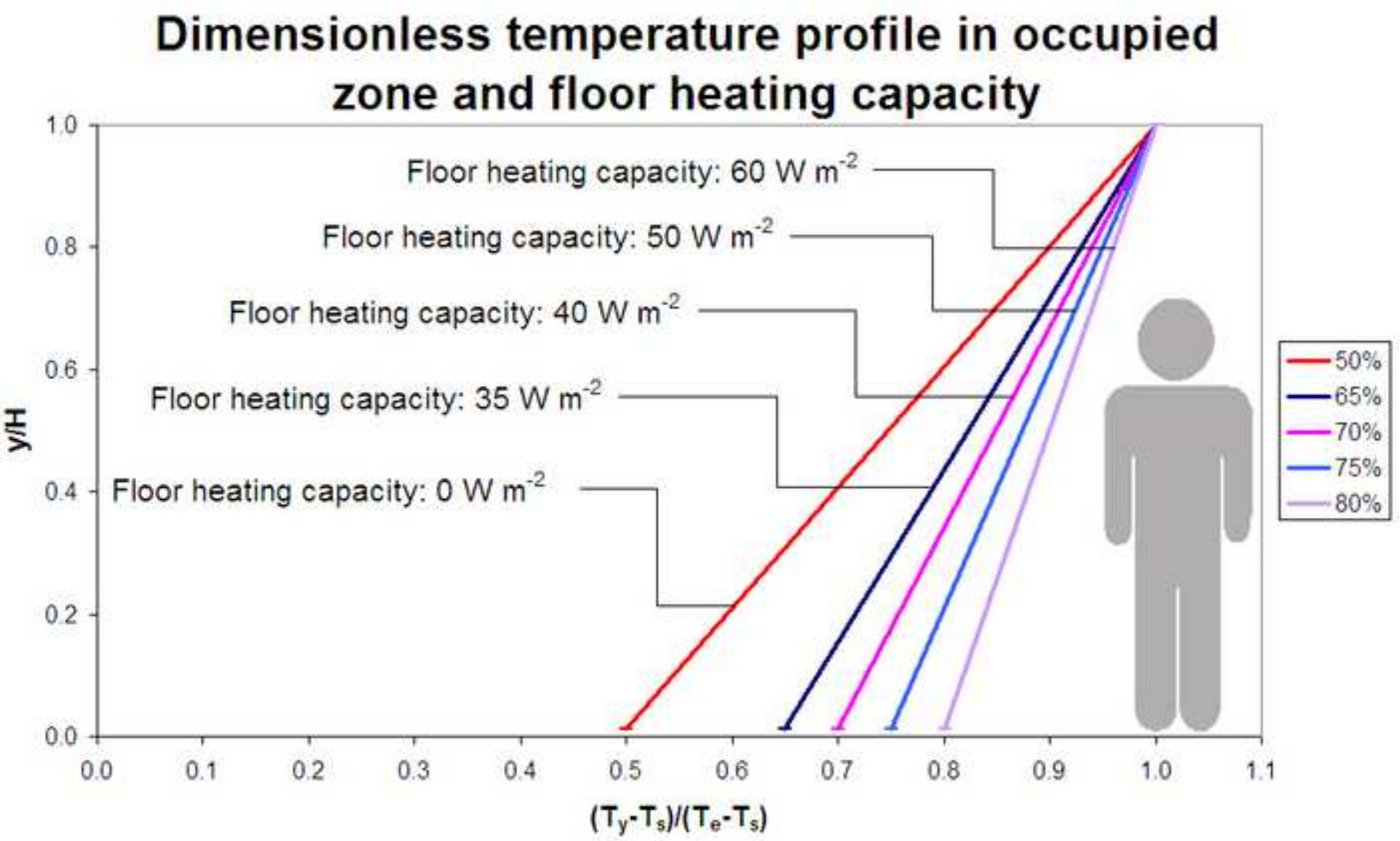
Dimensionless temperature profile in occupied zone and floor heating capacity
Floor heating capacity: 60 W m-2
Floor heating capacity: 50 W m-2
Floor heating capacity: 40 W m-2
Floor heating capacity: 35 W m-2
Floor heating capacity: 0 W m-2
50%
65%
70%
75%
80%
y/H
(Ty-Ts)/(Te-Ts)
0.0
0.2
0.4
0.6
0.8
1.0
0.1
0.3
0.5
0.7
0.9
1.1

Figure 10

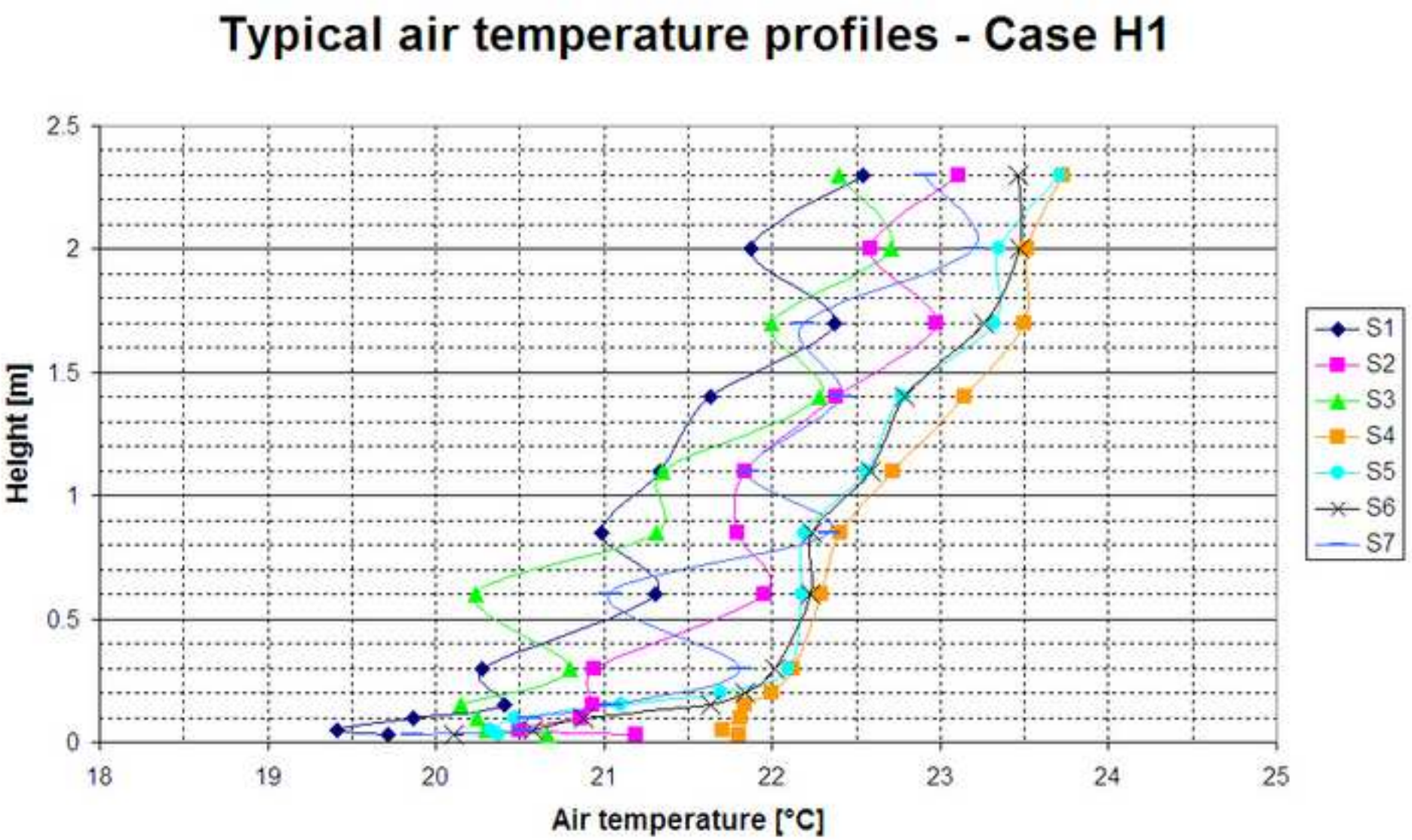
Typical air temperature profiles - Case H1
Height [m]
2.5
2
1.5
1
0.5
0
18
19
20
21
22
23
24
25
Air temperature [°C]
S1
S2
S3
S4
S5
S6
S7

Figure 11

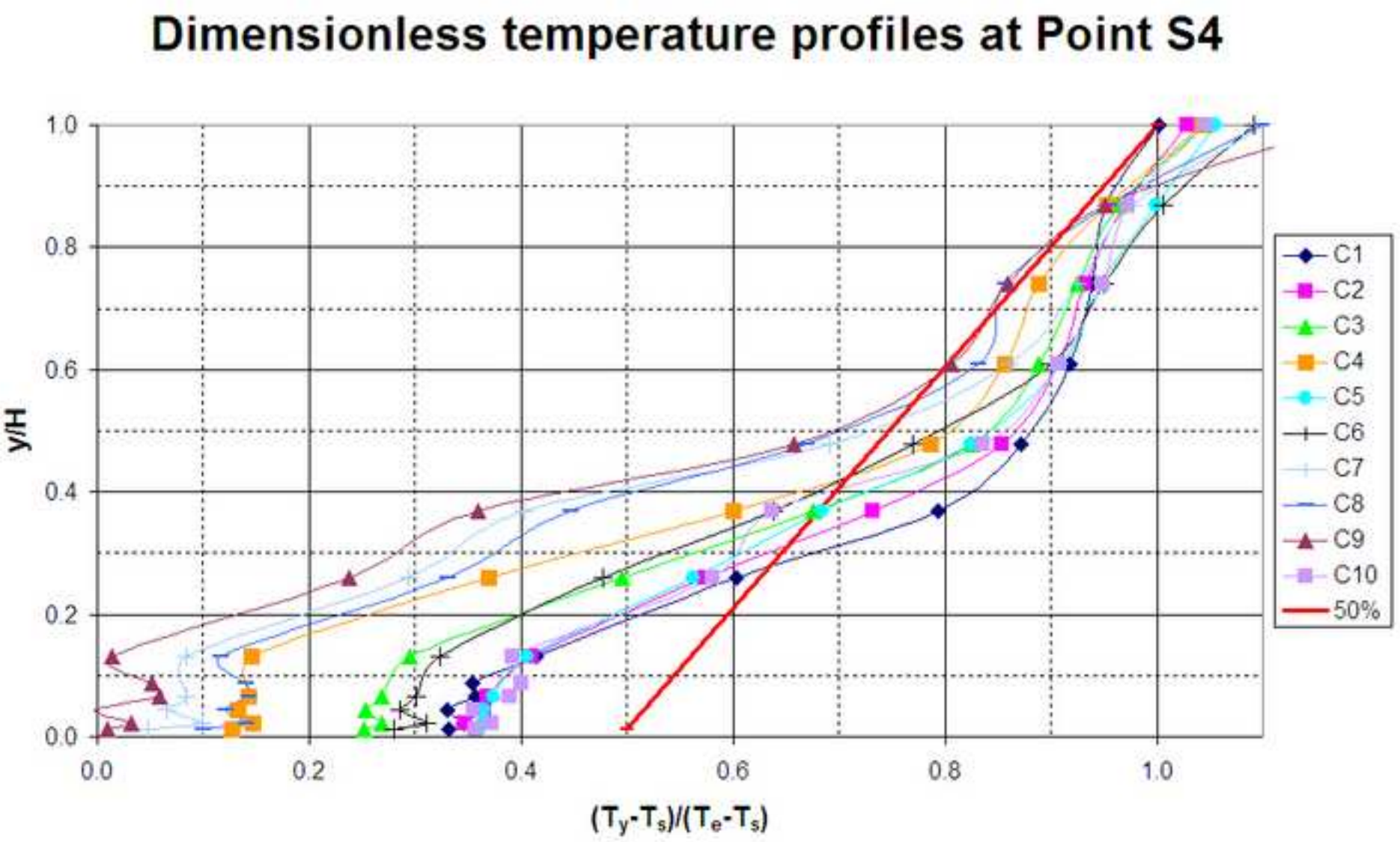
Dimensionless temperature profiles at Point S4
y/H
1.0
0.8
0.6
0.4
0.2
0.0
0.0
0.2
0.4
0.6
0.8
1.0
(Ty-Ts)/(Te-Ts)
C1
C2
C3
C4
C5
C6
C7
C8
C9
C10
50%

ACCEPTED MANUSCRIPT

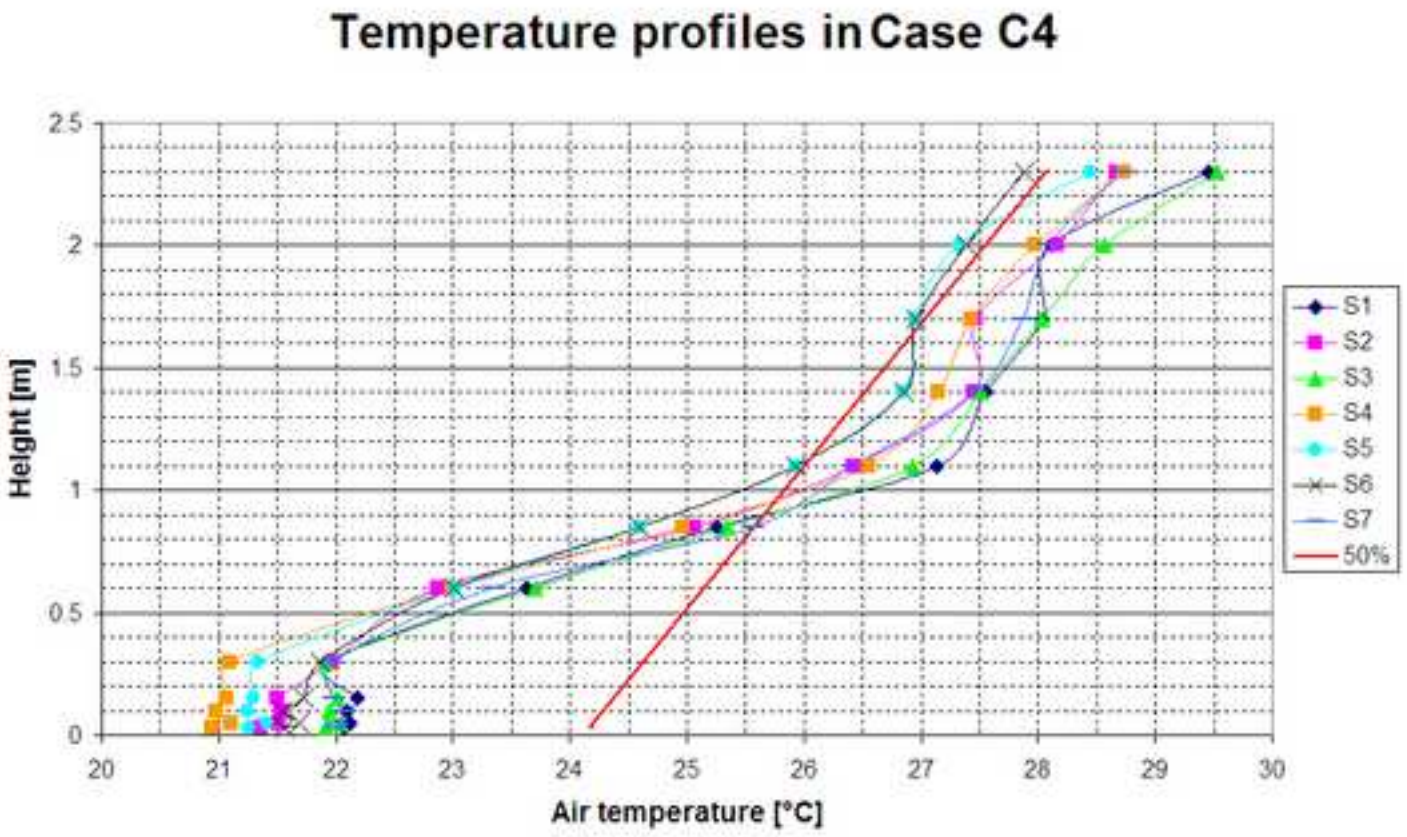

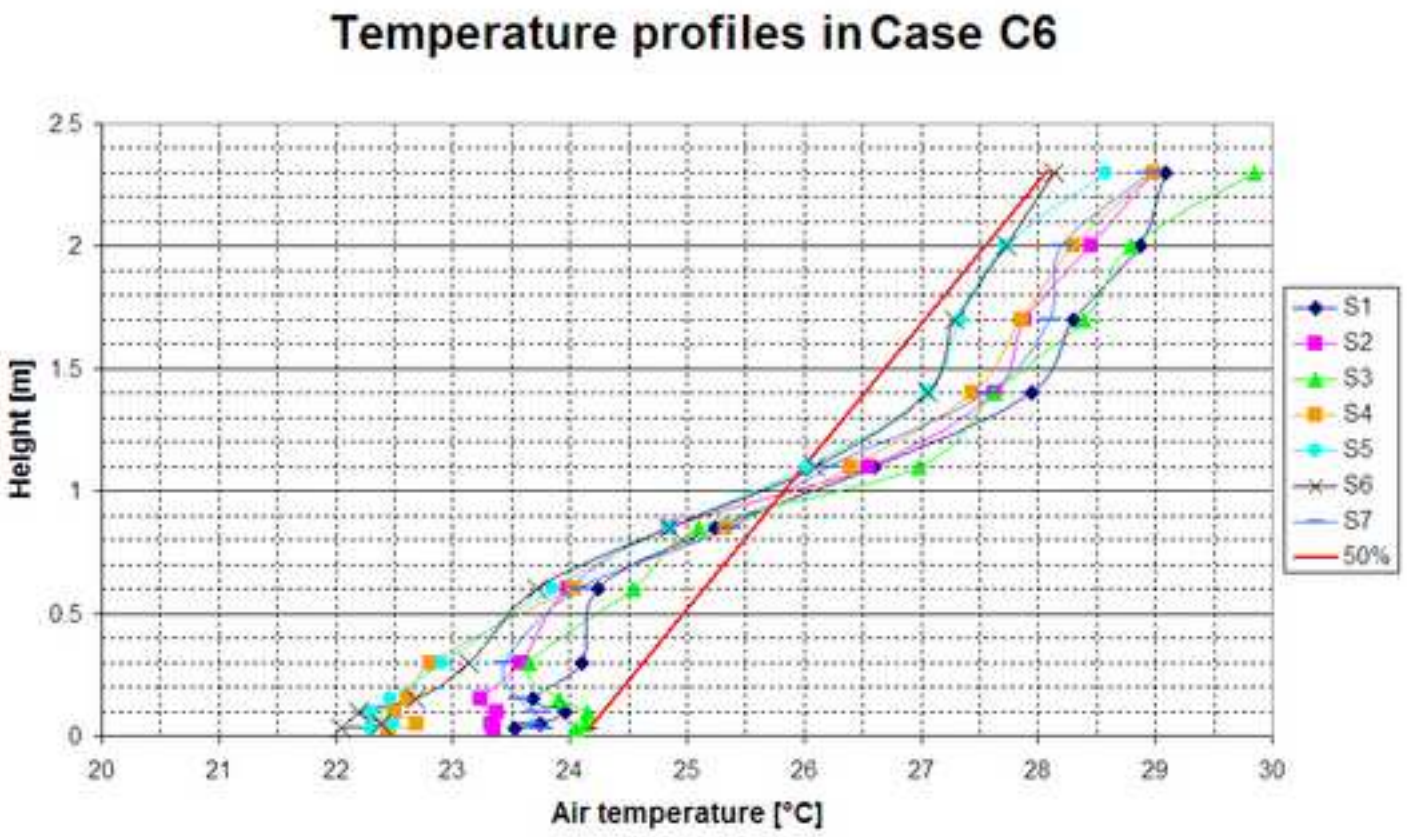

Figure 13

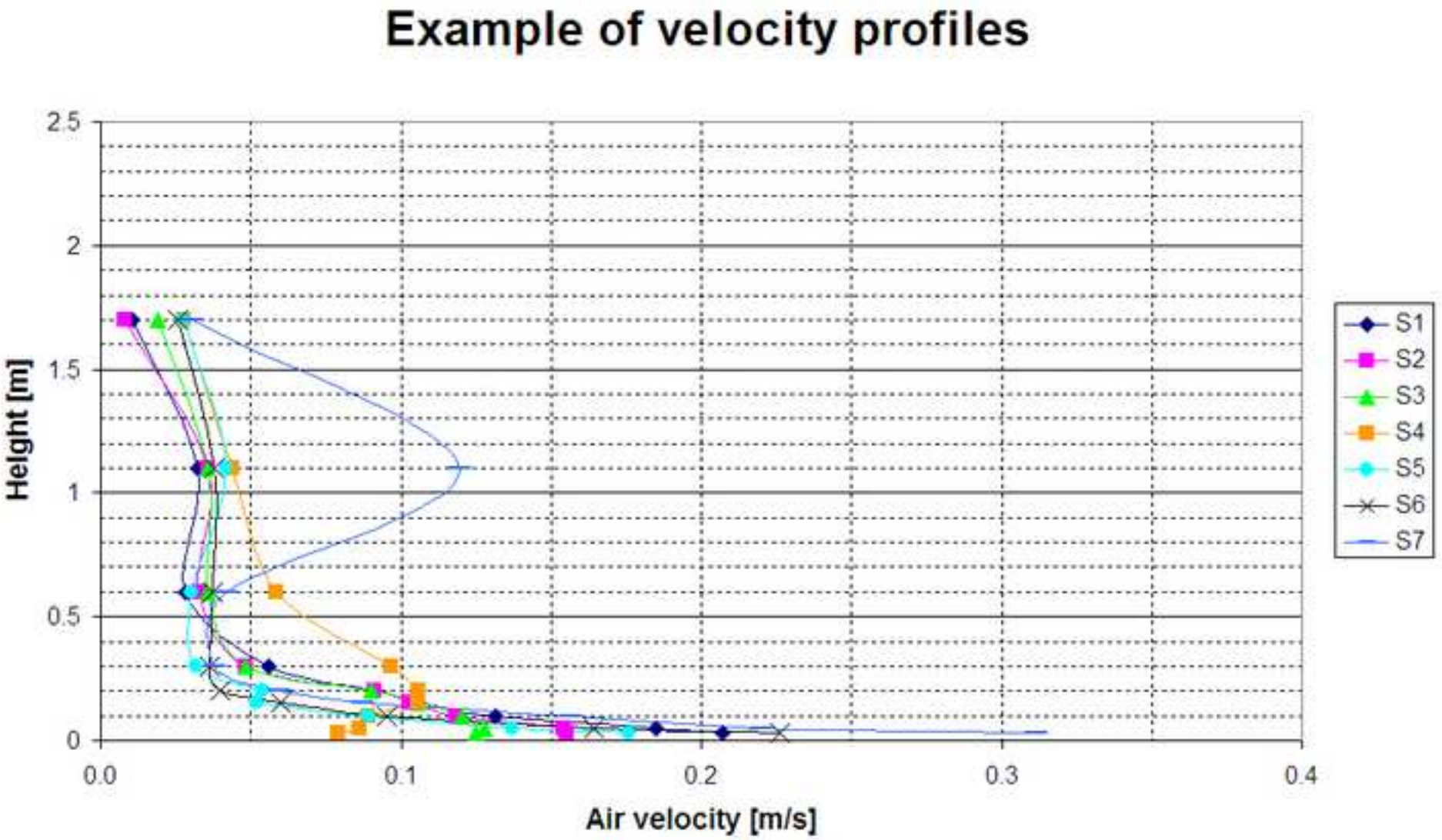
Example of velocity profiles
Height [m]
2.5
2
1.5
1
0.5
0
0.0
0.1
0.2
0.3
0.4
Air velocity [m/s]
S1
S2
S3
S4
S5
S6
S7

ACCEPTED MANUSCRIPT

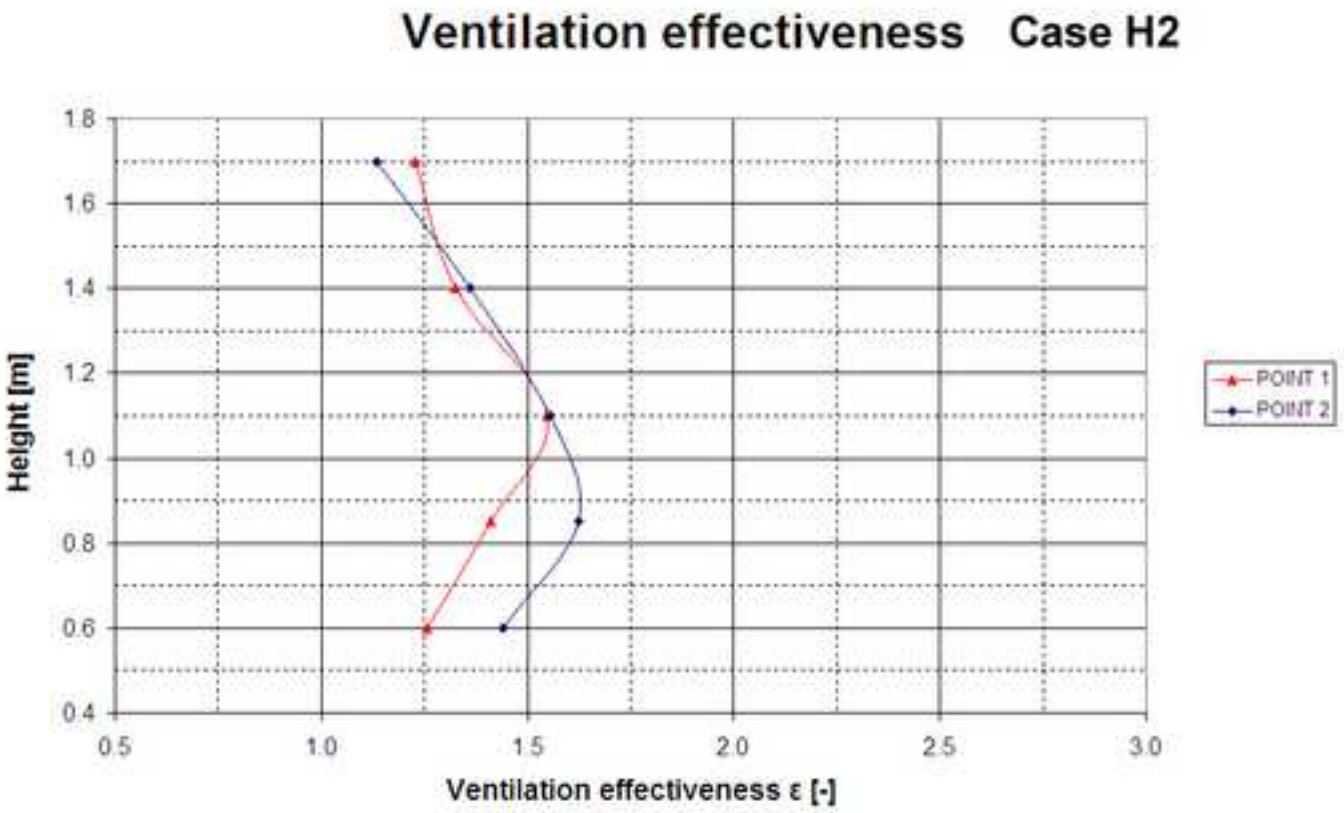

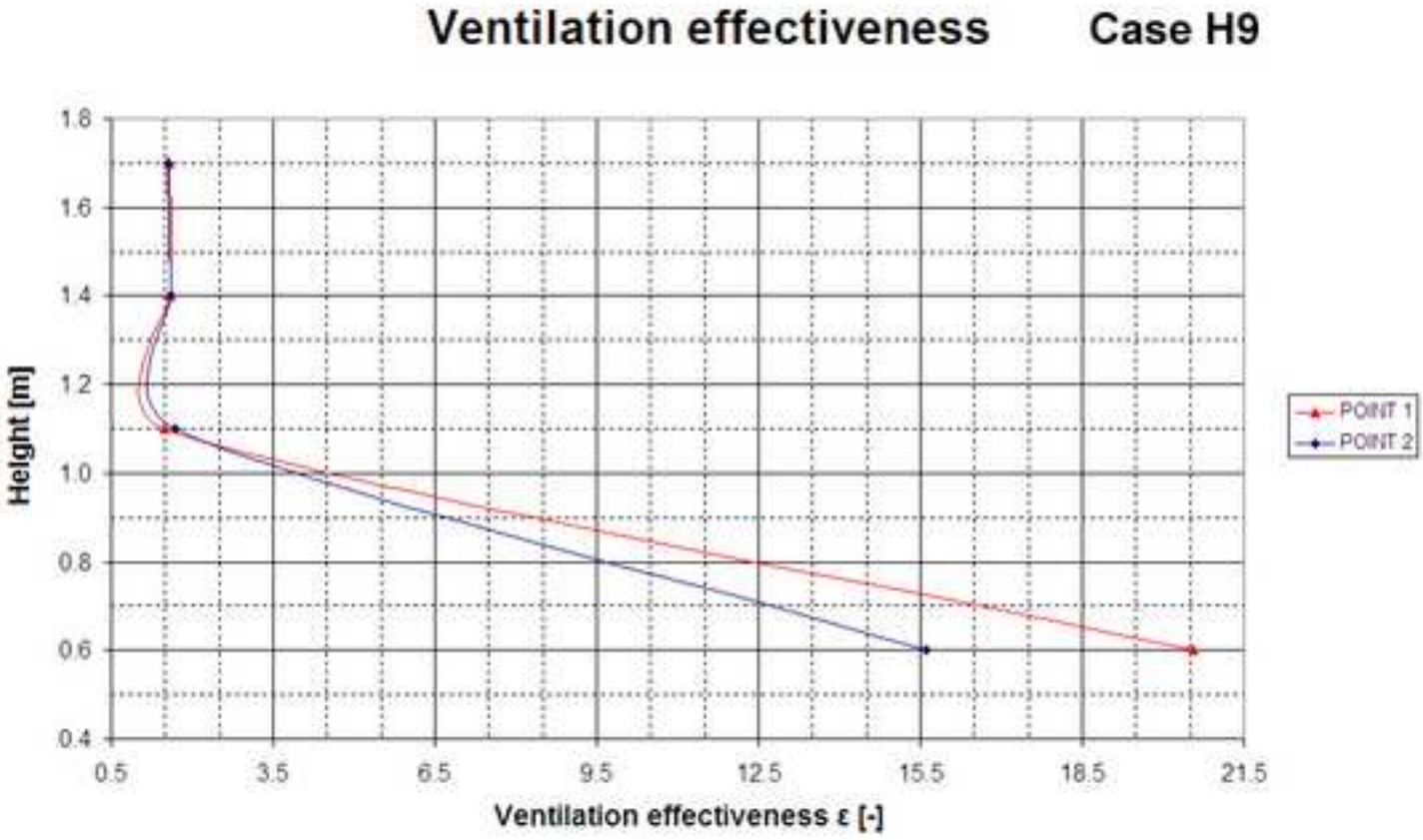

Figure 15

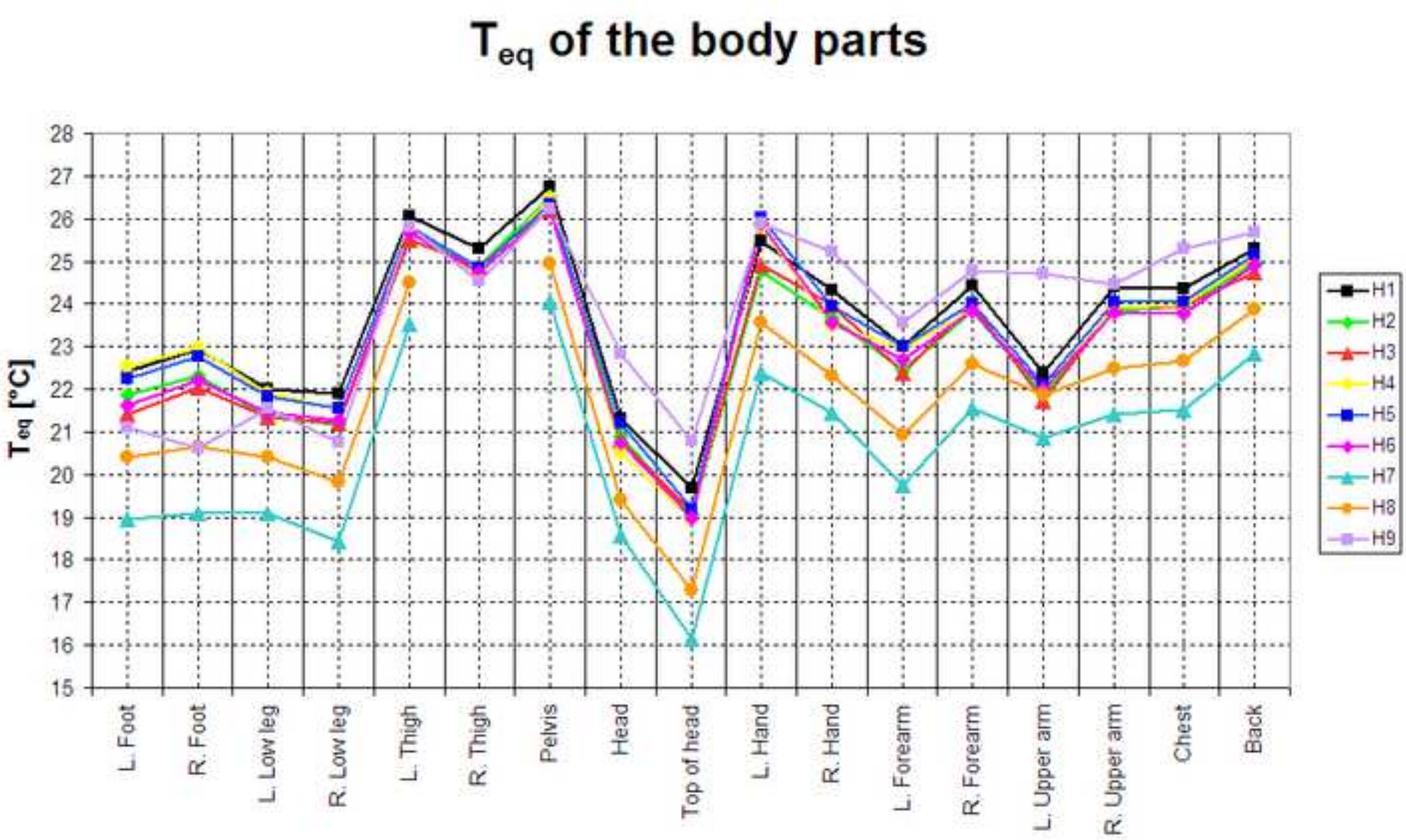
T_{eq} of the body parts
T_{eq} [°C]
28
27
26
25
24
23
22
21
20
19
18
17
16
15
L. Foot
R. Foot
L. Low leg
R. Low leg
L. Thigh
R. Thigh
Pelvis
Head
Top of head
L. Hand
R. Hand
L. Forearm
R. Forearm
L. Upper arm
R. Upper arm
Chest
Back
H1
H2
H3
H4
H5
H6
H7
H8
H9

Figure 16

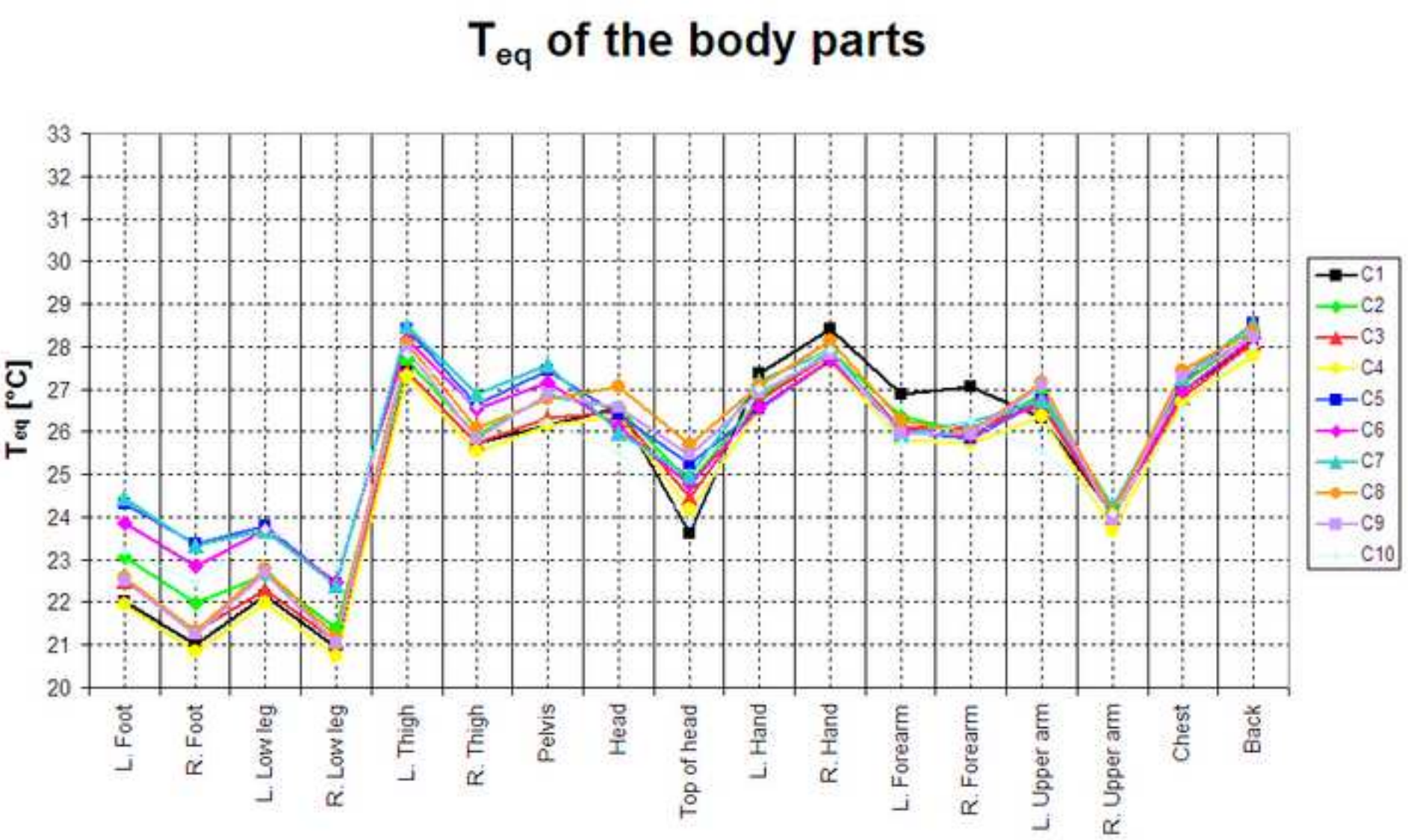
T_{eq} of the body parts
T_{eq} [°C]
33
32
31
30
29
28
27
26
25
24
23
22
21
20
L. Foot
R. Foot
L. Low leg
R. Low leg
L. Thigh
R. Thigh
Pelvis
Head
Top of head
L. Hand
R. Hand
L. Forearm
R. Forearm
L. Upper arm
R. Upper arm
Chest
Back
C1
C2
C3
C4
C5
C6
C7
C8
C9
C10